Article:
Hughes, D orcid.org/0000-0002-8004-8631 and Brummell, NH (2021) Double-Diffusive Magnetic Layering. The Astrophysical Journal, 922. 195. ISSN 0004-637X

https://doi.org/10.3847/1538-4357/ac2057

Draft version August 19, 2021
Typeset using LaTeX **twocolumn** style in AASTeX62

Double-Diffusive Magnetic Layering

D. W. Hughes[1] and N. H. Brummell[2]

[1]*Department of Applied Mathematics, University of Leeds, Leeds LS2 9JT, UK*
[2]*Department of Applied Mathematics, Baskin School of Engineering, University of California, Santa Cruz, CA 95064, USA*

ABSTRACT

Double-diffusive systems, such as thermosolutal convection, in which the density depends on two components that diffuse at different rates, are prone to both steady and oscillatory instabilities. Such systems can evolve into layered states, in which both components, and also the density, adopt a 'staircase' profile. Turbulent transport is enhanced significantly in the layered state. Here we exploit an analogy between magnetic buoyancy and thermosolutal convection in order to demonstrate the phenomenon of magnetic layering. We examine the long-term nonlinear evolution of a vertically-stratified horizontal magnetic field in the so-called 'diffusive regime', where an oscillatory linear instability operates. Motivated astrophysically, we consider the case where the viscous and magnetic diffusivities are much smaller than the thermal diffusivity. We demonstrate that diffusive layering can occur even for subadiabatic temperature gradients. Magnetic layering may be relevant for stellar radiative zones, with implications for the turbulent transport of heat, magnetic field and chemical elements.

Keywords: instabilities — magnetic buoyancy — solar tachocline — Sun: magnetic fields

1. INTRODUCTION

In an electrically conducting gas, under the influence of gravity, horizontal magnetic fields with strength varying with depth can become unstable to what is known as magnetic buoyancy instability (Newcomb 1961; Parker 1966). This instability has been studied in some detail, both in the linear and nonlinear regimes, particularly with respect to the breakup and escape of the toroidal field within the Sun (see, e.g., the review by Hughes 2007).

The simplest means of demonstrating magnetic buoyancy instability is through consideration of a plane parallel atmosphere containing a horizontal magnetic field that varies in strength with height, $\boldsymbol{B} = B(z)\hat{\boldsymbol{y}}$. **This may be regarded as a local Cartesian description of an azimuthal field in a spherical geometry**. **For ideal (non-diffusive) MHD**, Newcomb (1961) showed, via the energy principle, that necessary and sufficient conditions for instability are that somewhere in the plasma either

$$\frac{\mathrm{d}\rho}{\mathrm{d}z} > -\frac{\rho g}{a^2 + c^2}, \tag{1}$$

for modes for which the field lines do not bend (interchange modes), or

$$\frac{\mathrm{d}\rho}{\mathrm{d}z} > -\frac{\rho g}{c^2} \tag{2}$$

for three-dimensional (undular) perturbations with a very long wavelength in the direction of the imposed field. Here z is the vertical coordinate, increasing upwards, ρ is the density, g is the magnitude of the acceleration due to gravity, $a(z)$ and $c(z)$ are, respectively, the Alfvén speed and the adiabatic sound speed, defined by

$$a^2 = \frac{B^2}{\mu_0 \rho}, \qquad c^2 = \frac{\gamma p}{\rho}, \tag{3}$$

where p is the gas pressure, μ_0 is the magnetic permeability and γ is the usual ratio of specific heats.

The instability criteria (1) and (2) can be reformulated so that the role of the magnetic gradient is more evident (Thomas & Nye 1975), yielding

$$-\frac{ga^2}{c^2}\frac{\mathrm{d}}{\mathrm{d}z}\ln\left(\frac{B}{\rho}\right) > N^2 \tag{4}$$

for interchange modes, or

$$-\frac{ga^2}{c^2}\frac{\mathrm{d}}{\mathrm{d}z}\ln\left(B\right) > N^2 \tag{5}$$

Corresponding author: D.W. Hughes
d.w.hughes@leeds.ac.uk, brummell@soe.ucsc.edu

for undular modes, where

$$N^2 = \frac{g}{\gamma}\frac{\mathrm{d}}{\mathrm{d}z}\ln\left(p\rho^{-\gamma}\right) \tag{6}$$

is the square of the Brünt-Väisälä frequency, a measure of the stratification. Clearly, either a sufficiently rapid decrease with height of B/ρ or B can destabilize the interchange or undular modes respectively. It is of interest to note that, despite the stabilizing influence of magnetic tension, undular modes are more readily destabilized; the physics of the instability mechanism is discussed in Hughes & Cattaneo (1987).

The instability criteria (4) and (5) are derived assuming that there are no diffusive processes present (i.e. zero viscosity, resistivity and thermal diffusivity). The criteria are modified in a significant manner by the incorporation of magnetic and thermal diffusion (Gilman 1970; Acheson 1979). For example, for interchange modes, with horizontal and vertical wavenumbers k_x and k_z, the criterion for instability becomes

$$-\frac{ga^2}{c^2}\frac{\mathrm{d}}{\mathrm{d}z}\ln\left(\frac{B}{\rho}\right) > \frac{\eta}{\gamma\kappa}N^2 + \frac{\eta\nu}{\gamma}\frac{k^6}{k_x^2}, \tag{7}$$

where η is the magnetic diffusivity, κ the thermal diffusivity, ν the kinematic viscosity, and $k^2 = k_x^2 + k_z^2$. The effect of the ratio η/κ can be seen clearly by comparing conditions (4) and (7). For a given background subadiabatic stratification, a weaker gradient of magnetic field is required to promote instability when $\eta/\kappa < \gamma$. Essentially, for a perturbed parcel of fluid, the stabilizing effects of the thermal stratification are eroded more quickly by diffusive effects than the destabilizing effects of the magnetic stratification, and therefore instability is more likely to occur. In astrophysical contexts, $\eta \ll \kappa$ and thus the difference between criteria (4) and (7) is significant.

Criteria (1) and (2) (or (4) and (5)) describe the onset of direct (steady) instabilities. The incorporation of diffusion not only modifies these criteria (e.g. expression (7)), but also introduces another entire class of unsteady, oscillatory instabilities. The instability mechanism (which is described below) is more subtle, but can again be distilled into a criterion relating the gradient of B/ρ to the background stratification. As shown by Hughes (1985), the criterion for instability of interchange modes is

$$\begin{aligned} -\frac{ga^2}{c^2}\left(\eta+\nu-\kappa\left(\gamma-1\right)\right)\frac{\mathrm{d}}{\mathrm{d}z}\ln\left(\frac{B}{\rho}\right) > \\ \left(\kappa+\nu\right)\left(\kappa+\eta\right)\left(\eta+\nu\right)\frac{k^6}{k_x^2} + (\kappa+\nu)N^2. \end{aligned} \tag{8}$$

Of particular note here is that two very different forms of the field can be unstable, depending on the sign of the factor $\eta+\nu-(\gamma-1)\kappa$. For $\eta+\nu > (\gamma-1)\kappa$, instability occurs if B/ρ decreases sufficiently rapidly with height, whereas for $\eta+\nu < (\gamma-1)\kappa$, instability occurs if B/ρ increases sufficiently rapidly with height. The latter condition on the diffusion coefficients is readily satisfied in stellar interiors, and exhibits a conundrum whereby instability occurs owing to diffusive effects in a situation where both the thermodynamic and magnetic gradients individually appear to be stabilizing.

Much more is known about these types of instabilities outside of the magnetic context. Instabilities of a convectively stable state that arise owing to the disparate diffusion rates of two components that contribute to the density are generally known as *double-diffusive* instabilities. Double-diffusive systems have been studied extensively, chiefly motivated by their applications to oceanographical and astrophysical mixing; the field is reviewed in the monograph by Radko (2013). The two components contributing to the density are typically the temperature and a concentration field of some material fluid contaminant, in what are known as thermosolutal systems. The most well-studied example is that of the oceanographic thermohaline system (see, for example, the review by Schmitt 1994), where the two components are heat and salt, with cooler and saltier water being denser.

If hot, salty water overlies cold, fresh water in proportions such that the overall density stratification still has the density decreasing upwards, double-diffusive direct instability can occur, due to heat diffusing much faster than salt. A parcel of water displaced upwards loses its stabilizing (relatively cool) thermal content to its surroundings, but retains more of its destabilizing (relatively fresh) salinity content. It can thus be less dense than its surroundings — in this case, the perturbation therefore continues to move upwards (and vice versa for downward displacements). Sinusoidal perturbations elongate upwards and downwards and the direct instability in this case is often known as ‘salt fingering’ (or just ‘fingering’). The underlying mechanism of the steady magnetic buoyancy interchange instability, governed by criterion (7), may be described in an analogous fashion to that of salt fingers.

Conversely, if the situation is reversed, whereby cold, fresh water overlies hot, salty water, instability can still occur, but in an oscillatory, overstable manner. A parcel perturbed upwards is denser than its surroundings and so returns to its original position. Through diffusive exchange, it returns cooler but fresher than it was initially. If the net effect is such that the parcel is denser than its original form, then it will overshoot. The process thus repeats, leading to oscillations that grow with time. This situation is often known as the 'diffusive' form of the double-diffusive instability in the oceanographic context, or 'semi convection' in the astrophysical context (where the mean molecular weight of the gas content replaces the effect of salt). Note, however, as intimated above with regard to equation (8), the oscillatory form of the magnetic double-diffusive instability is rather subtle. In particular, unlike for thermohaline convection, it cannot necessarily simply be considered as a reversal of the stabilizing and destabilizing roles of the components in comparison with the direct instability. Most strikingly, for $\eta + \nu < (\gamma - 1)\kappa$, instability can occur when both the B/ρ and entropy $(p\rho^{-\gamma})$ gradients are stabilizing, as measured by the diffusionless criterion (4). As shown by Hughes (1985), in these circumstances the instability can still be interpreted in terms of a fluid parcel (or flux tube) argument, but with the key ingredient being the role played by the compressive heating of the magnetic field.

Double-diffusive instabilities — of both the fingering and diffusive types — are of particular interest because the motions they engender induce mixing where it might not be expected if one merely considers convective instabilities based on the overall density gradient. Enhanced thermal and saline transport in the oceans can contribute to the existence of large-scale circulations (e.g. Rahmstorf 2006), and anomalous chemical abundances in stars can be more consistent with double-diffusively enhanced transport there (e.g. Langer 1991).

One of the most intriguing aspects of double-diffusive convection is its tendency to form layers or 'staircases'. Importantly, further enhanced transport can result from a secondary instability leading to such layered states. These states are identified by their stepped salinity, temperature and density profiles with depth, representing well-mixed convective layers separated by steep-gradient interfaces. The formation of layers occurs for both the fingering and diffusive regimes, although there are differences in the two, particularly in the interface dynamics. Observations of both types of layering are found in the oceans: fingering staircases require overlying warm salty water, as in the tropical Atlantic (e.g. Schmitt et al. 2005), whereas diffusive staircases require overlying cold, fresh water, as found in the Arctic (e.g. Timmermans et al. 2008). For both regimes, it is found that the layered states have a measurably stronger vertical transport.

Many possible explanations have been advanced for the formation of layers. Merryfield (2000) reviewed the state of play of the theory of double-diffusive staircase formation, discussing in some detail the four main candidates proposed at that time: the collective instability of salt fingers (Stern 1969); the possibility of metastable equilibria; instability via negative density diffusion (cf. Phillips 1972; Posmentier 1977); intrusions resulting from horizontal gradients (e.g. Zhurbas & Ozmidov 1983). Subsequently, a fifth candidate has emerged — the so-called γ instability of Radko (2003). This may be characterized as a mean field instability, driven by gradients in the flux ratio γ, which can operate in both the fingering and diffusive regimes[1]. Somewhat of a resurgence has occurred in the theoretical understanding of layer formation, driven by the fact that computational technology has become powerful enough to accommodate the range of scales that seems necessary to simulate the process, and hence test possible theories of layer formation. The simulation of layer formation is computationally demanding for two reasons: it relies on a large range of spatial scales and, furthermore, it is, in some sense, a slow process. However, today's most powerful computers can overcome these constraints. Consequently, persuasive numerical simulations of layer formation in both the fingering and diffusive regimes have been performed (e.g. Stellmach et al. 2011; Rosenblum et al. 2011).

Given the importance of the layering process for turbulent transport in thermosolutal convection, coupled with the recent possibility of simulating layering computationally in the astrophysical context (see the comprehensive review by Garaud 2018), this raises the interesting question of whether magnetic buoyancy instabilities (a double-diffusive system, as discussed above) can also lead to layering and, if so, what are the implications for transport in magnetized stellar interiors? Under certain constraints, there is a direct analogy between the dynamics of magnetic buoyancy instabilities (including diffusion) and the well-studied thermohaline convection (Spiegel & Weiss 1982, see also Section 2). The formal transformation between the two systems holds in the magneto-Boussinesq limit and for two-dimensional motions in which, for the magnetic system, the field remains unidirectional. This transformation, however, does not map temperature and salinity gradients in the thermohaline system directly to entropy and magnetic field gradients in the magnetic buoyancy system, as one might naively expect. Whereas salt does map directly to magnetic pressure, temperature in the thermohaline problem maps to a linear combination of temperature and magnetic pressure in the magnetic buoyancy problem. Thus the results for magnetic buoyancy are, at first sight, a little surprising, particularly, as already noted,

[1] Note that γ in this context is not the ratio of the specific heats used earlier.

the occurrence of instability for 'stable' gradients of both entropy and magnetic field.

The aim of this paper is to exploit the analogy between the two systems, building on the new understanding of double-diffusive dynamics revealed in the oceanographic and astrophysical contexts, in order to take a first look at the nature of the layering that can occur as a result of magnetic buoyancy. Through the analogy we know that layering will occur, at some parameter values; the question is whether such parameters, on translation to the magnetic case, might match a relevant astrophysical regime. Stellar interiors are characterized by the regime $\nu < \eta \ll \kappa$ or, equivalently, $\sigma < \tau \ll 1$, where $\sigma = \nu/\kappa$ is the Prandtl number and $\tau = \eta/\kappa$ is the ratio of magnetic to thermal diffusivity. More precisely, at the base of the solar convection zone, for example, $\sigma \approx 2 \times 10^{-6}$ and $\tau \approx 3 \times 10^{-5}$ (see, e.g., Gough 2007). This is a long way from the oceanographic regime, for which the ratio of salt to heat diffusion $\tau \approx 10^{-2}$ and $\sigma \approx 7$. Indeed, whereas it is possible to simulate the oceanographic regime at the correct parameter values, this is a forlorn hope in astrophysics. The numerical evidence suggests that layering in the fingering regime ceases to occur for small σ, but is maintained in the diffusive regime (Mirouh et al 2012; Garaud 2018). For astrophysical implications, we therefore choose to concentrate on the diffusive regime. Furthermore, this allows us to study the possibility of layering in the regime where the gradients of both B/ρ and $p/\rho^{-\gamma}$ are positive (and hence stable in the absence of diffusion).

The layout of the paper is as follows. The mathematical problem, and specifically the link between the thermohaline and magnetic buoyancy systems, is formulated in § 2, for both bounded and unbounded domains. The linear instability theory of both systems is summarized in § 3. The detailed results of the nonlinear computations for two examples of the layering process are contained in § 4. A summary of our results, together with their astrophysical implications, is contained in § 5.

2. MATHEMATICAL FORMULATION

The aim of this section is to formulate the mathematical descriptions of both thermohaline convection and magnetic buoyancy and to describe how the systems can be mapped onto each other. As discussed in the introduction, the analogy between the two systems holds only in two dimensions; thus we shall, from the outset, restrict attention to this case. In § 2.1 and § 2.2 we shall consider, respectively, the general formulation of the equations of thermohaline convection and magnetic buoyancy. The case of unbounded domains, for both systems, is discussed in § 2.3.

2.1. *The Equations of Thermohaline Convection*

The basic state for Boussinesq thermohaline convection has uniform vertical (z) gradients in temperature and salinity, $\overline{T}_z$ and $\overline{S}_z$. We denote perturbations to the temperature and salinity of this state by T and S respectively; density perturbations ρ are then given by $\rho/\rho_0 = -\alpha_T T + \alpha_S S$, where ρ_0 is a representative density and α_T and α_S are (positive) expansion coefficients. We describe the two-dimensional, incompressible velocity $\boldsymbol{u} = (u, 0, w)$ in terms of a stream function $\psi(x, z, t)$, defined by $\boldsymbol{u} = \boldsymbol{\nabla} \times (\psi \hat{\boldsymbol{y}})$; the vorticity is then $\boldsymbol{\nabla} \times \boldsymbol{u} = \omega \hat{\boldsymbol{y}}$, with $\omega = -\nabla^2 \psi$. We scale lengths with d, a characteristic length of the system, times with d^2/κ, where κ is the thermal diffusivity, T with $-\overline{T}_z d$ and S with $-\overline{S}_z d$. Two-dimensional Boussinesq thermohaline convection is then governed by the following three dimensionless equations, describing, respectively, the evolution of the vorticity and the temperature and salinity perturbations (e.g. Turner 1973, noting that his ψ is the negative of our ψ):

$$\frac{1}{\sigma}\left(\frac{\partial\left(\nabla^2\psi\right)}{\partial t} + J\left(\psi, \nabla^2\psi\right)\right) = Ra\frac{\partial T}{\partial x} - Rs\frac{\partial S}{\partial x} + \nabla^4\psi, \tag{9}$$

$$\frac{\mathrm{D}T}{\mathrm{D}t} \equiv \frac{\partial T}{\partial t} + J\left(\psi, T\right) = \frac{\partial \psi}{\partial x} + \nabla^2 T, \tag{10}$$

$$\frac{\mathrm{D}S}{\mathrm{D}t} \equiv \frac{\partial S}{\partial t} + J\left(\psi, S\right) = \frac{\partial \psi}{\partial x} + \tau\nabla^2 S, \tag{11}$$

where the Jacobian J is defined by

$$J(f, g) = \frac{\partial f}{\partial x}\frac{\partial g}{\partial z} - \frac{\partial f}{\partial z}\frac{\partial g}{\partial x}. \tag{12}$$

The problem is governed by four dimensionless parameters: the thermal and solutal Rayleigh numbers, Ra and Rs, the Prandtl number σ and the diffusivity ratio τ are defined by

$$Ra = -\frac{g\alpha_T \overline{T}_z d^4}{\kappa\nu},\ Rs = -\frac{g\alpha_S \overline{S}_z d^4}{\kappa\nu},\ \sigma = \frac{\nu}{\kappa},\ \tau = \frac{\kappa_s}{\kappa}, \tag{13}$$

where g is the acceleration due to gravity, κ_s the solutal diffusivity, and ν the kinematic viscosity. In an experimental setup, the characteristic length d would represent the vertical distance between the two boundaries. With the Rayleigh numbers so defined, positive (negative) Ra is thermally destabilizing (stabilizing), whereas positive (negative) Rs is solutally stabilizing (destabilizing).

2.2. *The Equations of Magnetic Buoyancy*

We shall consider the equations of magnetic buoyancy under the magneto-Boussinesq approximation derived by Spiegel & Weiss (1982) (see also Corfield 1984;

Bowker et al. 2014). Under the 'standard' Boussinesq approximation (Spiegel & Veronis 1960), density variations appear only in the buoyancy term; in addition, to leading order, they result only from temperature variations, with variations in the gas pressure assumed to be negligible. In studies of magnetoconvection (see, e.g., the monograph by Weiss & Proctor 2014), the direct relation between density and temperature perturbations remains: the magnetic field plays no role in this balance. By contrast, the very essence of magnetic buoyancy instability is the influence of the magnetic field on the pressure; this is captured within the magneto-Boussinesq approximation through an ordering in which variations in the *total* pressure (i.e. gas + magnetic) are negligible, but variations in the gas pressure and magnetic pressure individually are not. Density variations are again taken into account only in the buoyancy term, and the velocity field is again assumed to be incompressible ($\boldsymbol{\nabla}\cdot\boldsymbol{u}=0$).

The basic state is taken to be magnetohydrostatic, with a horizontal, depth-dependent magnetic field $\boldsymbol{B}=B(z)\hat{\boldsymbol{y}}$, confined to a layer of depth d; the magneto-Boussinesq approximation requires that d is much smaller than the pressure and density scale heights. We consider two-dimensional (y-independent) perturbations in which the magnetic field remains unidirectional (so-called interchange modes), and again employ a stream function $\psi(x,z,t)$ with $\boldsymbol{u}=\boldsymbol{\nabla}\times(\psi\hat{\boldsymbol{y}})$.

Following the formulation of Spiegel & Weiss (1982), the vorticity equation may be written in dimensional terms as

$$\frac{\mathrm{D}}{\mathrm{D}t}\left(\nabla^2\psi\right)=\frac{g}{T_0}\frac{\partial\delta T}{\partial x}+\frac{g}{p_0}\frac{\partial\delta p_m}{\partial x}+\nu\nabla^4\psi, \qquad (14)$$

where δT and δp_m are the perturbations of temperature and magnetic pressure, and where a subscript zero denotes a representative value. Forming the scalar product of the induction equation with the magnetic field gives

$$\frac{\mathrm{D}\delta p_m}{\mathrm{D}t}=-\alpha\frac{\partial\psi}{\partial x}+\eta\nabla^2\delta p_m, \qquad (15)$$

where

$$\alpha=\frac{B_0^2}{\mu_0}\frac{\mathrm{d}}{\mathrm{d}z}\ln\left(\frac{B}{\rho}\right). \qquad (16)$$

On adopting the ordering $\delta p_m\approx-\delta p$ (negligible variation in total pressure), the energy equation becomes

$$\frac{\mathrm{D}}{\mathrm{D}t}\left(\delta T+\frac{\delta p_m}{C_p\rho_0}\right)=-\beta\frac{\partial\psi}{\partial x}+\kappa\nabla^2\delta T, \qquad (17)$$

where C_p is the specific heat at constant pressure and

$$\beta=\frac{T_0}{\gamma}\frac{\mathrm{d}}{\mathrm{d}z}\ln\left(\frac{p}{\rho^\gamma}\right) \qquad (18)$$

is the subadiabatic temperature gradient (treated as constant within the Boussinesq approximation).

Equation (15) is already in standard advection-diffusion form (cf. equations (10), (11)). Although equation (17) is not, equations (15) and (17) can be combined to give

$$\frac{\mathrm{D}\delta T^*}{\mathrm{D}t}=-\beta^*\frac{\partial\psi}{\partial x}+\kappa\nabla^2\delta T^*, \qquad (19)$$

where

$$\delta T^*=\delta T-\frac{\tau\delta p_m}{C_p\rho_0(1-\tau)},\quad \beta^*=\beta-\frac{\alpha}{C_p\rho_0(1-\tau)}, \qquad (20)$$

and where now $\tau=\eta/\kappa$. On employing the scalings

$$\delta p_m=-S\alpha d,\qquad \delta T^*=-T\beta^* d, \qquad (21)$$

together with the standard non-dimensionalization of lengths with d and times with d^2/κ, equations (15) and (19) become (11) and (10) respectively. Since, in this formulation, the underlying gradients are β^* and α, the associated Rayleigh numbers are

$$Ra_m=-\frac{gd^4\beta^*}{\kappa\nu T_0},\quad Rs_m=\frac{gd^4\alpha}{\kappa\nu p_0}. \qquad (22)$$

The dimensionless form of equation (14) is then transformed into equation (9) through the mapping

$$Ra=Ra_m,\qquad Rs=\frac{(\gamma-\tau)}{\gamma(1-\tau)}Rs_m. \qquad (23)$$

For completeness, it is also instructive to present the set of dimensionless equations describing magnetic buoyancy without applying any transformation. As discussed in the introduction, consideration solely of the magnetic buoyancy problem shows that instability results from a competition between gradients of B/ρ and $p\rho^{-\gamma}$ (e.g. equation (4) or (7)). With this in mind, for this case we therefore use α, defined by (16), and β, defined by (18), in the non-dimensionalization. On adopting the usual scalings of lengths with d, times with d^2/κ, and writing

$$\delta T=-\beta d\,\widetilde{\delta T},\qquad \delta p_m=-\alpha d\,\widetilde{\delta p_m}, \qquad (24)$$

the dimensionless forms of equations (14), (17) and (15) become, on dropping tildes,

$$\frac{1}{\sigma}\frac{\mathbf{D}}{\mathbf{D}t}\left(\nabla^2\psi\right)=Rt\frac{\partial\delta T}{\partial x}-Rb\frac{\partial\delta p_m}{\partial x}+\nabla^4\psi, \qquad (25)$$

$$\frac{\mathbf{D}\delta T}{\mathbf{D}t}-\left(\frac{\gamma-1}{\gamma}\right)\left(\frac{Rb}{Rt}\right)\frac{\mathbf{D}\delta p_m}{\mathbf{D}t}=\frac{\partial\psi}{\partial x}+\nabla^2\delta T, \qquad (26)$$

$$\frac{\mathbf{D}\delta p_m}{\mathbf{D}t} = \frac{\partial \psi}{\partial x} + \tau \nabla^2 \delta p_m, \quad (27)$$

where, as in Hughes & Proctor (1988), the thermal and magnetic Rayleigh numbers are defined by

$$Rt = -\frac{g d^4 \beta}{\kappa \nu T_0}, \quad Rb = \frac{g d^4 \alpha}{\kappa \nu p_0}. \quad (28)$$

From expressions (22), (23) and (28), together with the definition of β^*, it follows that Rt and Rb are linked to Ra and Rs via the linear relations

$$Ra = Rt + \frac{(\gamma - 1)}{\gamma(1-\tau)} Rb, \quad Rs = \frac{(\gamma - \tau)}{\gamma(1-\tau)} Rb. \quad (29)$$

We have already seen how, through the transformation (20), the equations of magnetic buoyancy may be transformed into those of thermohaline convection. Alternatively, if we let

$$\delta\Sigma = \frac{\delta p_m}{\alpha}, \qquad \delta\lambda = \alpha \delta T + \left(\frac{\alpha}{C_p \rho_0} - \beta \right) \delta p_m, \quad (30)$$

then (26) and (27) can be expressed as

$$\frac{\mathbf{D}\delta\Sigma}{\mathbf{D}t} = -\frac{\partial \psi}{\partial x} + \eta \nabla^2 \delta\Sigma, \quad (31)$$

and

$$\frac{\mathbf{D}\delta\lambda}{\mathbf{D}t} = \kappa \nabla^2 \delta\lambda + \tilde{\kappa} \nabla^2 \delta\Sigma, \quad (32)$$

where $\tilde{\kappa} = \alpha\kappa(\beta - 1/C_p\rho_0)$. Thus within this framework, magnetic buoyancy may also be viewed as a binary fluid with cross-diffusion (see, e.g., Batiste et al. 2006). However, it is worth stressing that the transformed variables δT^*, defined by (20), and $\delta\lambda$, defined by (30), are only helpful when δT and δp_m obey the same boundary conditions.

For clarity, it is worth recapping the rationale behind the three related systems parameterized by (Ra, Rs), (Ra_m, Rs_m) or (Rt, Rb). Equations (9)–(11) describe thermohaline convection. The transformation (20), with associated Rayleigh numbers given by (22), leads to a set of equations of a very similar form to (9)–(11): the further transformation of Rayleigh numbers (23) recovers (9)–(11) exactly. The third system (25)–(27) results from retaining δT and δp_m as variables and scaling with the 'natural' gradients arising from considerations of diffusionless magnetic buoyancy, namely α and β, leading to the Rayleigh numbers given by (28). Under this formulation, expression (26) is not in standard advection-diffusion form, thereby leading to counter-intuitive behavior when interpreting this system.

2.3. *Unbounded Domains*

In the analysis of oceanic thermohaline convection, it is reasonable to assume that the upper and lower boundaries play no significant role, and hence to consider a vertically unbounded fluid layer (e.g. Stern & Radko 1998). Indeed, it is within such systems that the most interesting nonlinear phenomena are observed computationally.

The basic state for thermohaline convection is again characterized by a uniform temperature gradient $\overline{T}_z$ and a uniform salinity gradient $\overline{S}_z$. In the absence of any boundaries, we adopt the lengthscale d defined by $d^4 = |\kappa\nu/g\tilde{\alpha}\overline{T}_z|$, i.e. the lengthscale obtained by setting the absolute value of the local Rayleigh number equal to unity. Various possible scalings for T and S may be adopted: here we choose to scale (dimensional) T and S by $T = d|\overline{T}_z|\hat{T}$, $S = d(\tilde{\alpha}/\tilde{\beta})|\overline{T}_z|\hat{S}$. On dropping hats, the dimensionless governing equations for the perturbations of the basic state are

$$\frac{1}{\sigma}\frac{\mathrm{D}}{\mathrm{D}t}\left(\nabla^2\psi\right) = \frac{\partial T}{\partial x} - \frac{\partial S}{\partial x} + \nabla^4\psi, \quad (33)$$

$$\frac{\mathrm{D}T}{\mathrm{D}t} = -\mathrm{sgn}(\overline{T}_z)\frac{\partial \psi}{\partial x} + \nabla^2 T, \quad (34)$$

$$\frac{\mathrm{D}S}{\mathrm{D}t} = -\mathrm{sgn}(\overline{S}_z)\frac{1}{R_0}\frac{\partial \psi}{\partial x} + \tau\nabla^2 S, \quad (35)$$

where the density ratio $R_0 = |\tilde{\alpha}\overline{T}_z/\tilde{\beta}\overline{S}_z| = |Ra/Rs|$. Note that by our definition, R_0 is always positive; from our choice of scalings for T and S, the signs of the temperature and salinity gradients enter explicitly in equations (34) and (35), but not in (33). It can be seen that in an unbounded domain, for given σ and τ, the dynamics is controlled simply by the ratio of the Rayleigh numbers (i.e. R_0), together with the signs of the basic state gradients. Finally, we note that scaling the dimensional density ρ with $\tilde{\alpha} d|\overline{T}_z|\rho_0$ gives the following expression for the dimensionless density:

$$\rho = \left(\frac{\mathrm{sgn}(\overline{S}_z)}{R_0} - \mathrm{sgn}(\overline{T}_z) \right) z + S - T. \quad (36)$$

It should be noted, e.g. from expression (36), that in an unbounded domain with linear gradients of T, S and ρ, these quantities can take negative values, depending on the range of z considered. This has no physical significance: it is only gradients that matter, not the absolute values of T, S or ρ.

In extended astrophysical systems, it is again reasonable to downplay the role of boundaries and thus, similarly, to consider infinite domains for the study of magnetic buoyancy instability. On adopting $d =$

$|\kappa\nu T_0/g\beta^*|^{1/4}$ as the unit of length, scaling δT^* and δp_m as

$$\delta T^* = |\beta^*|d\,\widetilde{\delta T^*}, \qquad \delta p_m = |\beta^*|d\frac{p_0}{T_0}\widetilde{\delta p_m}^*, \tag{37}$$

and defining the density ratio R_1 by

$$R_1 = \frac{|\beta^*|p_0}{|\alpha|T_0}, \tag{38}$$

the dimensionless governing equations may be expressed, after dropping the tildes, as

$$\frac{1}{\sigma}\frac{\mathrm{D}}{\mathrm{D}t}\left(\nabla^2\psi\right) = \frac{\partial\delta T^*}{\partial x} + \frac{(\gamma-\tau)}{\gamma(1-\tau)}\frac{\partial\delta p_m}{\partial x} + \nabla^4\psi, \tag{39}$$

$$\frac{\mathrm{D}\delta T^*}{\mathrm{D}t} = -\mathrm{sgn}(\beta^*)\frac{\partial\psi}{\partial x} + \nabla^2\delta T^*, \tag{40}$$

$$\frac{\mathrm{D}\delta p_m}{\mathrm{D}t} = -\mathrm{sgn}(\alpha)\frac{1}{R_1}\frac{\partial\psi}{\partial x} + \tau\nabla^2\delta p_m. \tag{41}$$

Equations (33)–(35) are thus recovered on making the identifications

$$T = \delta T^*, \quad S = -\frac{(\gamma-\tau)}{\gamma(1-\tau)}\delta p_m, \quad \frac{1}{R_0} = \frac{1}{R_1}\frac{(\gamma-\tau)}{\gamma(1-\tau)},$$
$$\mathrm{sgn}(\overline{T}_z) = \mathrm{sgn}(\beta^*), \qquad \mathrm{sgn}(\overline{S}_z) = -\mathrm{sgn}(\alpha). \tag{42}$$

Whereas for thermosolutal convection the crucial gradients are those of T and S, for magnetic buoyancy they are $p\rho^{-\gamma}$ and B/ρ. After some manipulation, and scaling consistent with the above (see the Appendix), these quantities take the dimensionless form

$$\frac{p}{\rho^\gamma} = \text{const.} + \left(\mathrm{sgn}(\beta^*)\gamma + \frac{\mathrm{sgn}(\alpha)}{R_1}\frac{(\gamma-1)}{(1-\tau)}\right)z + \gamma\delta T^* + \frac{(\gamma-1)}{(1-\tau)}\delta p_m \tag{43}$$

and

$$\frac{B}{\rho} = \text{const.} + \frac{\mathrm{sgn}(\alpha)}{R_1}z + \delta p_m. \tag{44}$$

In terms of perturbations from the background state, the key quantities are therefore the magnetic pressure variation δp_m and the variation of $p\rho^{-\gamma}$ (related to the entropy variation), which we shall denote by δs and which is given by

$$\delta s = \gamma\delta T^* + \frac{(\gamma-1)}{(1-\tau)}\delta p_m. \tag{45}$$

Although, for thermosolutal convection, the density is related in a simple manner to the temperature and salinity fields via expression (36), for the magnetic buoyancy system the relation between the two pivotal scalar fields and the density is not so straightforward. Indeed, as shown in the Appendix, it is possible to calculate only the deviation of the density from a reference hydrostatic state: after appropriate scaling, this deviation, $\hat{\rho}$ say, takes the dimensionless form

$$\hat{\rho} = -\left(\mathrm{sgn}(\beta^*) + \frac{(\gamma-\tau)}{\gamma(1-\tau)}\frac{\mathrm{sgn}(\alpha)}{R_1}\right)z - \delta T^* - \frac{(\gamma-\tau)}{\gamma(1-\tau)}\delta p_m. \tag{46}$$

It may also be noted that an alternative, possibly more intuitive, scaling for the equations of magnetic buoyancy is to adopt $d = |\kappa\nu T_0/g\beta|^{1/4}$ as the unit of length. On scaling δT and δp_m by

$$\delta T = |\beta|d\,\widetilde{\delta T}, \qquad \delta p_m = |\beta|d\frac{p_0}{T_0}\widetilde{\delta p_m}, \tag{47}$$

the dimensionless governing equations become, on dropping tildes,

$$\frac{1}{\sigma}\frac{\mathrm{D}}{\mathrm{D}t}\left(\nabla^2\psi\right) = \frac{\partial\delta T}{\partial x} + \frac{\partial\delta p_m}{\partial x} + \nabla^4\psi, \tag{48}$$

$$\frac{\mathrm{D}\delta T}{\mathrm{D}t} + \frac{(\gamma-1)}{\gamma}\frac{\mathrm{D}\delta p_m}{\mathrm{D}t} = -\mathrm{sgn}(\beta)\frac{\partial\psi}{\partial x} + \nabla^2\delta T, \tag{49}$$

$$\frac{\mathrm{D}\delta p_m}{\mathrm{D}t} = -\mathrm{sgn}\,(\alpha)\,\frac{1}{R_2}\frac{\partial\psi}{\partial x} + \tau\nabla^2\delta p_m, \tag{50}$$

where $R_2 = |\beta|p_0/|\alpha|T_0$.

To summarize for unbounded systems (as we did for finite domains), we have derived three different systems governing the double-diffusive behavior. The three systems are parameterized, separately, by R_0, R_1 and R_2; they are related, respectively, to those parameterized by (Ra, Rs), (Ra_m, Rs_m) and (Rt, Rb), discussed in § 2.2. The parameter R_0 is the density ratio in thermohaline convection, with governing equations (33)–(35). The R_1 system, where R_1 is directly proportional to R_0, is governed by equations (39)–(41) and arises from transforming the magnetic buoyancy equations into those of classical double-diffusive convection. The R_2 system, governed by equations (48)–(50), results from retaining the standard variables of magnetic buoyancy.

2.4. *Numerical Techniques*

We solve the governing equations of thermohaline convection, (33)–(35), numerically, and then use the transformations (42)–(46) to translate the results into the magnetic buoyancy system in the diffusive regime. In the absence of physical boundaries, we adopt periodic boundary conditions for the perturbations in both the horizontal and vertical directions. The equations are solved by a standard pseudo-spectral technique, with a 2/3 de-aliasing rule; time stepping is performed by combining a second-order Adams-Bashforth scheme with exponential time differencing.

3. LINEAR INSTABILITIES

The linear instabilities resulting from thermohaline convection and magnetic buoyancy have been extensively studied (see, e.g., the reviews by Turner 1973; Hughes 2007). Here we give a brief summary, both for completeness and also as necessary background for the nonlinear results described in Section 4.

3.1. *Bounded Domains*

Let us first consider thermohaline convection in a bounded system, governed by the linearized versions of equations (9)–(11). Instability can occur either as a steady or an oscillatory mode (e.g. Turner 1973). Steady convection, in the fingering regime, occurs via an exchange of stabilities when

$$Ra > Ra^{(e)} = \frac{Rs}{\tau} + \frac{k^6}{k_x^2}, \tag{51}$$

where, as earlier, k_x and k_z are the horizontal and vertical wavenumbers and $k^2 = k_x^2 + k_z^2$. Oscillatory convection, in the diffusive regime, occurs when

$$Ra > Ra^{(o)} = \left(\frac{\sigma+\tau}{1+\sigma}\right) Rs + \frac{(1+\tau)(\sigma+\tau)}{\sigma}\frac{k^6}{k_x^2}, \tag{52}$$

provided that

$$Rs > \frac{\tau^2(1+\sigma)}{\sigma(1-\tau)}\frac{k^6}{k_x^2}; \tag{53}$$

condition (53) guarantees that there is a real frequency of oscillation when $Ra = Ra^{(o)}$. The regions of linear stability and instability in the (Ra, Rs) plane for $\tau < 1$, together with the line of neutral buoyancy, are sketched in Figure 1(a). The onset of steady convection is predominantly in the third quadrant in the (Rs, Ra) plane, that of oscillatory convection entirely in the first quadrant.

The stability boundaries given by (51) and (52) can be translated into the (Rb, Rt) plane via the transformation (29), to give

$$Rt^{(e)} = \frac{Rb}{\tau} + \frac{k^6}{k_x^2}, \tag{54}$$

$$Rt^{(o)} = \frac{(1+\sigma+\tau-\gamma)}{\gamma(1+\sigma)} Rb + \frac{(1+\tau)(\sigma+\tau)}{\sigma}\frac{k^6}{k_x^2}. \tag{55}$$

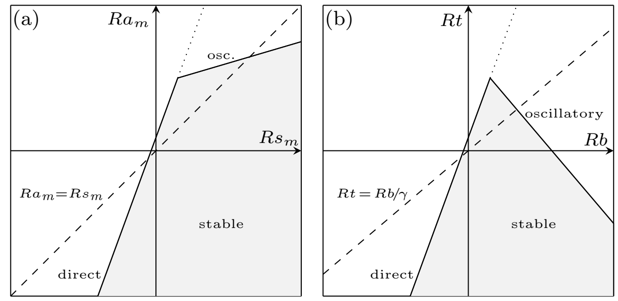

Figure 1. Sketches showing the regimes of linear instability in (a) the (Rs_m, Ra_m) plane (for $\tau < 1$) and (b) the (Rb, Rt) plane (for $\tau < \gamma - 1 - \sigma$). The lines of steady and oscillatory bifurcations are marked, together with the line of neutral buoyancy ($Ra_m = Rs_m$ in (a), $Rt = Rb/\gamma$ in (b)).

Note that the criteria for direct (steady) instability, (51) and (54), are identical in the (Ra, Rs) and (Rt, Rb) systems. The criteria for oscillatory instability, (52) and (55), however differ significantly. Expression (55) is the dimensionless form of (8): as discussed in the Introduction, and shown in Figure 1(b), it describes the appearance, for $\sigma + \tau < \gamma - 1$, of instability when Rt is negative and Rb positive — i.e. instability in the quadrant in which, in the absence of diffusion, both the thermal and magnetic (B/ρ) gradients are stabilizing.

3.2. *Unbounded Domains*

In an unbounded system it is natural to seek perturbations that are periodic in both the horizontal and vertical directions. It is convenient to express the stability criteria in terms of R_0^{-1}. The critical value of R_0^{-1} for steady convection is given by

$$\left(R_0^{-1}\right)^{(e)} = \mathrm{sgn}(\overline{S}_z)\tau\left(\mathrm{sgn}(\overline{T}_z) + \frac{k^6}{k_x^2}\right), \tag{56}$$

and that for oscillatory convection by

$$\left(R_0^{-1}\right)^{(o)} = \mathrm{sgn}(\overline{S}_z)\left(\mathrm{sgn}(\overline{T}_z)\left(\frac{1+\sigma}{\sigma+\tau}\right) + \frac{(1+\sigma)(1+\tau)}{\sigma}\frac{k^6}{k_x^2}\right), \tag{57}$$

provided also that

$$\frac{k^6}{k_x^2} < \mathrm{sgn}(\overline{T}_z)\frac{\sigma(1-\tau)}{(\sigma+\tau)}. \tag{58}$$

For $\tau < 1$, steady convection (fingering) chiefly occurs when the temperature gradient is stabilizing and the solutal gradient destabilizing. In this case, from (56), there is instability when

$$R_0^{-1} > \tau\left(1 + \frac{k^6}{k_x^2}\right). \tag{59}$$

Periodic boundary conditions allow modes that are independent of height z — so-called ‘elevator modes’, with

$k_z = 0$. From (59), these are the most readily destabilized modes, with $k_x \to 0$.

Oscillatory (diffusive) modes, on the other hand, occur when the temperature gradient is destabilizing and the solutal gradient stabilizing, leading, from (57), to instability when

$$R_0^{-1} < \frac{1+\sigma}{\sigma+\tau} - \frac{(1+\sigma)(1+\tau)}{\sigma}\frac{k^6}{k_x^2}. \tag{60}$$

As for the steady mode, the most readily destabilized oscillatory mode is an elevator mode ($k_z = 0$) with $k_x \to 0$. It should though be noted that in the unstable regime, away from marginal stability, the mode of maximum growth rate — for steady and oscillatory modes — takes a finite value of k_x.

Through the use of the transformation (29), it is straightforward to show that the region of instability in the $Rt < 0$, $Rb > 0$ quadrant is delineated by the following inequalities:

$$\frac{\gamma-\tau}{\gamma-1} < R_0^{-1} < \frac{1+\sigma}{\sigma+\tau}. \tag{61}$$

The condition for there to be a finite range of R_0^{-1} satisfying these inequalities (i.e. that the left hand side of inequality (61) is less than the right hand side) may be expressed as

$$(1-\tau)\left(\gamma-(1+\sigma+\tau)\right) > 0, \tag{62}$$

in accord with expression (55).

The instability criteria may alternatively be expressed in terms of R_1^{-1} or R_2^{-1}. For $\alpha < 0$ and $\beta^* > 0$, steady convection occurs if

$$R_1^{-1} > \frac{\gamma\tau(1-\tau)}{(\gamma-\tau)}\left(1+\frac{k^6}{k_x^2}\right), \tag{63}$$

and, with $\alpha > 0$ and $\beta^* < 0$, oscillatory convection occurs if

$$R_1^{-1} < \frac{\gamma(1-\tau)}{(\gamma-\tau)}\left(\frac{1+\sigma}{\sigma+\tau} - \frac{(1+\sigma)(1+\tau)}{\sigma}\frac{k^6}{k_x^2}\right). \tag{64}$$

Expressions (63) and (64) are straightforward scalings of (59) and (60).

In terms of R_2^{-1}, for $\alpha < 0$ and $\beta > 0$, steady convection occurs if

$$R_2^{-1} > \tau\left(1+\frac{k^6}{k_x^2}\right), \tag{65}$$

and, with $\alpha > 0$ and $\beta > 0$ (both gradients 'stabilizing'), oscillatory convection occurs if

$$R_2^{-1} > \frac{\gamma(1+\sigma)}{(\gamma-(1+\sigma+\tau))}\left(1+\frac{(1+\tau)(\sigma+\tau)}{\sigma}\frac{k^6}{k_x^2}\right), \tag{66}$$

provided that $\sigma+\tau < \gamma-1$. In transforming between the formally identical criteria (63) and (65) (or between (64) and (66)), it should be noted that k^6/k_x^2 is scaled with β^* for the expressions involving R_1 and with β for those involving R_2. **We note also the somewhat counter-intuitive difference in the inequalities (64) and (66); this arises since, in the unstable region of the $Rt < 0$, $Rb > 0$ quadrant,**

$$R_1 = \frac{(\gamma-1)}{\gamma(1-\tau)} - R_2. \tag{67}$$

4. MAGNETIC LAYERING

In this section, we discuss two representative cases of layer formation in the diffusive regime, in a domain of width 100π and height 200π. We solve the governing equations of thermohaline convection in an unbounded domain, (33)–(35), and relate these to the magnetic buoyancy system via the transformations (42). Motivated astrophysically, we adopt the smallest values of the Prandtl number σ and the diffusivity ratio τ compatible with long-time runs in large domains; as such, we set $\sigma = \tau = 0.01$. To accommodate the fine-scale structure, 2048×4096 spectral modes are used. Note, from (60), that oscillatory instability then occurs for $R_0^{-1} < 50.5$ $\left(R_1^{-1} < 50.297\right)$, and, from (61), that instability in the fourth (i.e. 'stable-stable') quadrant in the (R_b, R_t) plane occurs in the range $2.485 < R_0^{-1} < 50.5$ $\left(2.475 < R_1^{-1} < 50.297\right)$. We consider in detail two particular values of the background stratification parameter: $R_0^{-1} = 1.5$, which lies in the first quadrant of Figure 1(b), and $R_0^{-1} = 4$, which lies in the fourth. Since the underlying system that we solve computationally is that of thermohaline convection, we quote nice round numbers for R_0^{-1}; since τ is small, R_1^{-1} is very slightly smaller than R_0^{-1}. The initial condition for both sets of simulations consists of 20 elevator modes, together with a small random perturbation. These modes are essentially the fastest growing modes for $R_0^{-1} = 4$ and are about 1.5 times narrower than the fastest growing mode for $R_0^{-1} = 1.5$; the long-term evolution though is not dependent on the precise form of the initial conditions.

4.1. *The case of* $R_0^{-1} = 1.5$ $\left(R_1^{-1} = 1.494\right)$

Figure 2 shows the early evolution of the kinetic energy. Initially the kinetic energy grows in an oscillatory fashion, representative of the linear instability in the diffusive regime. The exponentially growing elevator modes are also exact solutions to the fully nonlinear equations, since the Jacobian terms in equations (9)–(11) vanish identically. They are though unstable once

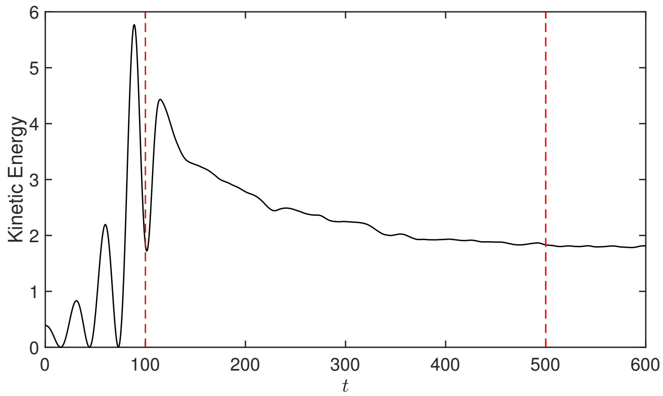

Figure 2. Kinetic energy as a function of time, during the initial instability phase: $R_0^{-1} = 1.5$. The dashed lines denote the times of the snapshots in Figures 3(a,b).

they attain sufficiently large amplitude; snapshots of ω, δs and δp_m during the break-up of the elevators are displayed in Figure 3(a). The nonlinear evolution of this secondary instability causes a rapid and total disruption of the elevators, as shown by the snapshots in Figure 3(b). All memory of the elevators is lost and the system is characterized by small-scale vorticity, together with small-scale entropy and magnetic pressure perturbations; at this stage, the mean profiles of p/ρ^γ, B/ρ and ρ remain essentially linear, as shown in Figure 4.

Following a period of equilibration ($100 \lesssim t \lesssim 1000$), in which the kinetic energy is stationary, the trend for the kinetic energy (although subject to sizeable short-term fluctuations) is an inexorable gradual increase, as shown in Figure 5. Associated with this rise in kinetic energy is the gradual emergence of a layered state from the homogeneous turbulence, and its subsequent evolution. Figure 3(c) shows the four-layered states in δs and δp_m at $t = 3600$, with the latter more pronounced, owing to the small value of τ. The layering in the vorticity ω is much less distinct. The interfaces between the layers are highly turbulent and mobile, with jets of fluid penetrating the interfaces and eventually leading to their destruction.

Figure 6(a) shows ω, δs and δp_m at $t = 8050$, where now only three layers remain; indeed, it can be seen from the figure that the upper layer is already disintegrating under turbulent erosion. Figure 6(b) shows the corresponding plots at $t = 11700$, at which point only two layers remain. The staircase structure in p/ρ^γ, B/ρ and ρ associated with the layers can be seen clearly in Figure 7(a), which plots the horizontal averages of these quantities at the times corresponding to Figures 3(c), 6(a,b).

One of the most significant features of the layering process in double-diffusive convection is the increase in the vertical turbulent flux of the two diffusing components; this feature is illustrated by the thermohaline simulations of Stellmach et al. (2011) in the fingering regime and those of Mirouh et al (2012) in the diffusive regime. As shown in Figure 8, for the thermohaline problem, the fluxes of both heat and salt are positive (upwards) in the diffusive regime. It thus follows immediately that the flux of δp_m will be negative. It is though not obvious *a priori* what the sign of the entropy flux will be, since, from (42) and (45),

$$\langle w\,\delta s\rangle = \gamma\langle wT\rangle - \frac{\gamma(\gamma-1)}{(\gamma-\tau)}\langle wS\rangle, \qquad (68)$$

with $\langle wT\rangle$ and $\langle wS\rangle$ both positive, and where $\langle\cdot\rangle$ denotes a global average. In the turbulent regime considered here, $\langle wT\rangle$ and $\langle wS\rangle$ are of comparable magnitude, as shown in Figure 8, and hence, since τ is small, $\langle w\,\delta s\rangle \approx \langle wT\rangle \approx \langle wS\rangle$. As the layering proceeds, the fluxes increase in magnitude, whilst becoming much more noisy. Between the quasi-stationary phase when the flow is homogeneous (following the instability of the initial finger modes) and $t = 11700$ (corresponding to Figure 6(b)) there is an approximate five-fold increase in the turbulent fluxes. **Note that the ratio of these two average turbulent fluxes defines the "γ" of the "γ-instability" in the mean-field theory of the cause of layering in thermohaline double-diffusive convection (Radko 2003): $\gamma = \langle wT\rangle/\langle wS\rangle$. A study of the variation of this γ with R_0 (or rather γ^{-1} with R_0^{-1}) is required to determine whether the theory fits our results, but this effort lies beyond the scope of this paper.**

4.2. *The case of* $R_0^{-1} = 4$ $\left(R_1^{-1} = 3.984\right)$

Here we consider the evolution from an equilibrium state for which both the magnetic field and the entropy gradient may, at least in the absence of diffusion, be considered to be stable (i.e. B/ρ and p/ρ^γ both increasing with height). In terms of the natural parameters for the magnetic problem (Rt and Rb), the presence of instability is somewhat surprising. However, viewed in terms of the transformed parameters (22), there is no particular significance to the line $Rt = 0$; as discussed above, it simply corresponds to $R_0^{-1} = (\gamma-\tau)/(\gamma-1) = 2.485$ here.

In its broad aspects, the evolution for $R_0^{-1} = 4$ is similar to that of $R_0^{-1} = 1.5$. Following the growth and saturation of the linear instability, there is a persistent yet noisy increase of kinetic energy, as shown in Figure 9. Comparison of Figures 5 and 9 shows that the increased stratification leads to a reduced growth rate

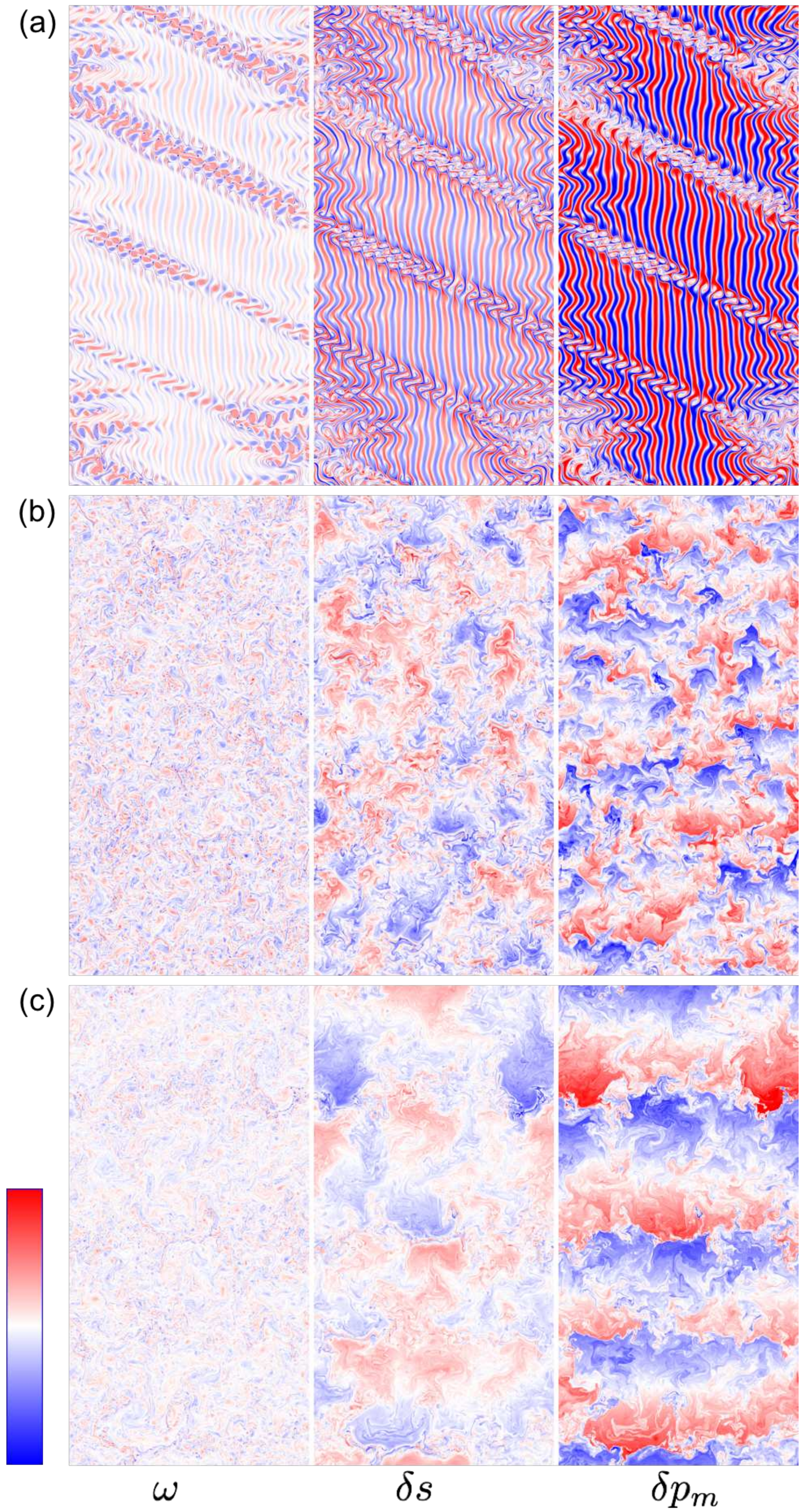

Figure 3. Snapshots at (a) $t = 100$, (b) $t = 500$ and (c) $t = 3600$ of ω, δs and δp_m (all scaled independently) for the case of $R_0^{-1} = 1.5$. The color table ranges from blue (largest negative value) to red (largest positive value), with white denoting the zero value.

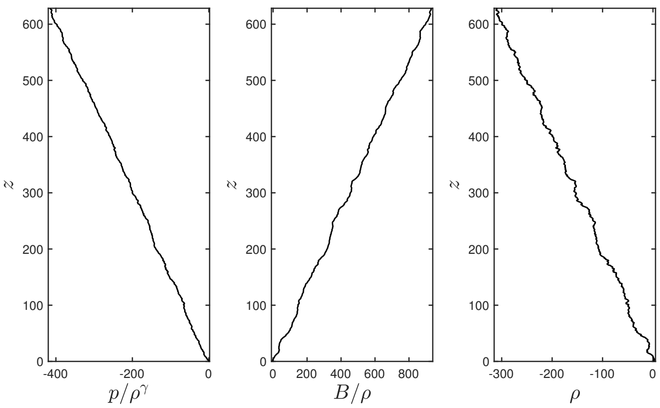

Figure 4. Horizontally averaged profiles of p/ρ^γ, B/ρ and ρ versus height at $t = 500$; $R_0^{-1} = 1.5$.

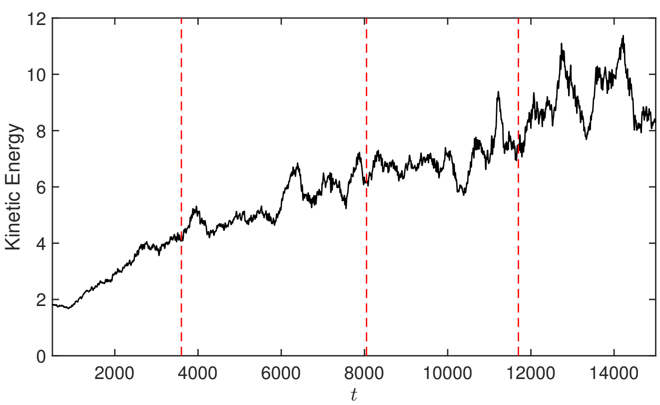

Figure 5. Kinetic energy as a function of time, for $t > 500$: $R_0^{-1} = 1.5$. The dashed lines denote the times of the snapshots in Figures 3c, 6a,b.

of the kinetic energy. Figure 10 shows that, after the initial linear instability of the elevators and the subsequent breakup into smaller-scale turbulence, layers form by eroding the regions of turbulence, as for the evolution for $R_0^{-1} = 1.5$, albeit now on a slower timescale. Figure 10(c) shows the evolution shortly after the layering process has extended across the entire domain. In comparison with the first distinct staircase to emerge for the case of $R_0^{-1} = 1.5$ (see Figure 3), the staircase for $R_0^{-1} = 4$ has shallower steps; furthermore, the flow between the interfaces is less turbulent, leading to a more coherent staircase structure.

Of particular note is the structure of the staircase and its relation to that of the equivalent thermohaline system. Figure 11 shows, for the same time as shown in Figure 10(c), the horizontally averaged profiles of p/ρ^γ, B/ρ and ρ, together with the corresponding profiles of T, S and ρ for the thermohaline problem. In the latter, the background temperature gradient is destabilizing, whereas the salinity gradient is stabilizing. As expected, the staircase structure is more sharply defined in S than T, owing to the small value of the diffusivity ratio τ. For the magnetic buoyancy problem, the profile of B/ρ is related to that of S via the transformations (42) and (44); indeed, for small τ, B/ρ is essentially $-S$. The most striking feature of Figure 11 is the sharpness and structure of the profile in p/ρ^γ. Since here the mean entropy gradient is 'stabilizing' (p/ρ^γ increasing with height), convection can occur only through a local reversal (or reversals) of this gradient. Hughes & Weiss (1995) examined this phenomenon in their explanation of steady convection in the regime with $Rt < 0$ and $Rb < 0$ for a fluid confined by rigid boundaries. In that case, the role of the boundary layers is paramount, with the strong field in the magnetic boundary layers leading to an exceptionally stable entropy gradient in the boundary layers. To compensate, there is of necessity a negative (destabilizing) entropy gradient across the remainder of the cell; this is such as to drive steady convection. Here, in an unbounded domain, a staircase is formed in which there are weakly unstable entropy gradients between the interfaces and strongly stable gradients across the interfaces themselves.

Figure 12 shows that the layering process again leads to a marked overall increase in turbulent transport, but with significant short-term fluctuations; the fluxes are about one fifth of their values for $R_0^{-1} = 1.5$. It is of interest to note that, as for the case of $R_0^{-1} = 1.5$, the balance $\langle w\,\delta s\rangle \approx \langle wT\rangle \approx \langle wS\rangle > 0$ still holds, even though the background entropy gradient is now positive. Although we see no layer merger in the very long run we have performed, we envisage, based on the results from other simulations of thermohaline convection, that at yet longer times the layers would eventually merge, ultimately giving only one step.

Three-dimensional thermosolutal simulations of the two cases we have considered have been performed by Mirouh et al (2012), who find the existence of layers for $R_0^{-1} = 1.5$ but not for $R_0^{-1} = 4$. This discrepancy between our results and theirs for the case of $R_0^{-1} = 4$ may be a genuine difference between two and three dimensions, or may be a result of the facts that (a) our two-dimensional simulations were performed at much higher resolution than the three-dimensional cases, and (b) our two-dimensional cases were integrated for much longer than was possible for the three-dimensional runs, thus allowing layered states eventually to emerge.

5. DISCUSSION

The purpose of this paper has been to expand ideas related to the mixing processes available in stars. Often, the inferred information about the interiors of stars

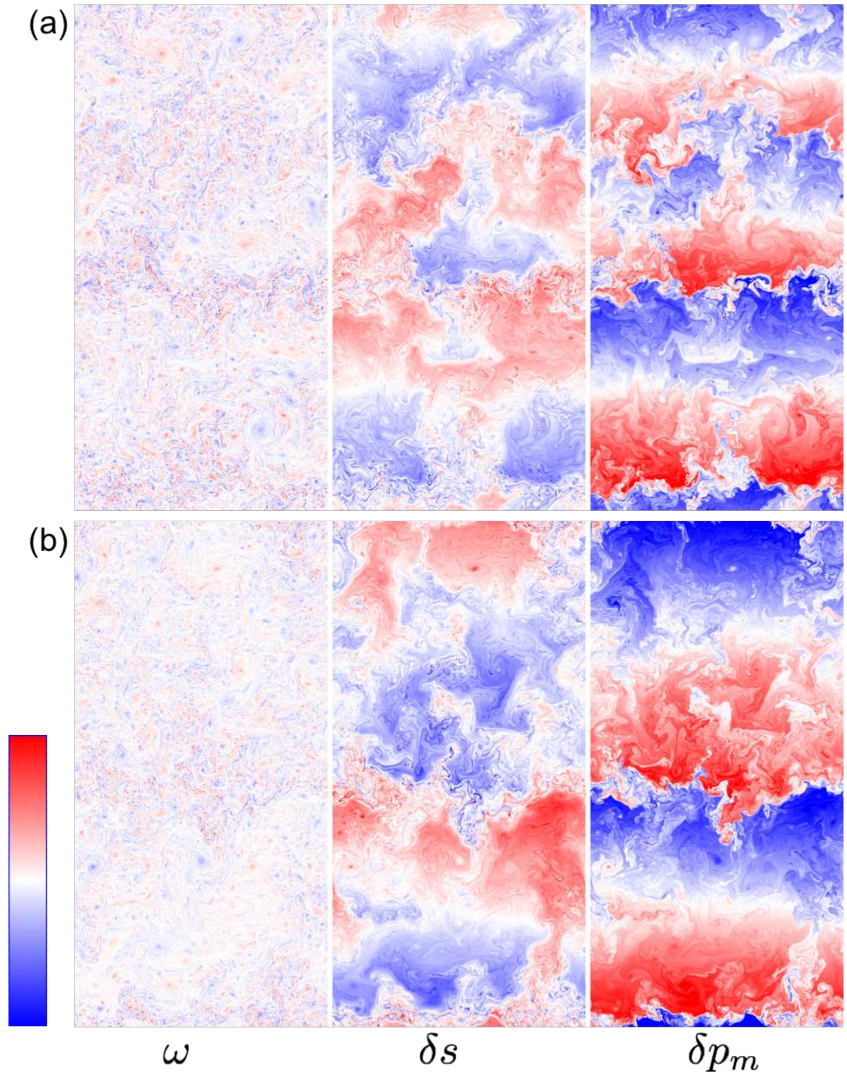

Figure 6. Snapshots at (a) $t = 8050$ and (b) $t = 11700$ of of ω, δs and δp_m (all scaled independently) for the case of $R_0^{-1} = 1.5$. The color table ranges from blue (largest negative value) to red (largest positive value), with white denoting the zero value.

gleaned from observations reveals that our knowledge of mixing processes therein is incomplete. For example, when helioseismology probed the interior rotation profile of the Sun, it revealed the tachocline, raising new challenges to our understanding of solar angular momentum transport. Similarly, the long-standing issue regarding solar lithium abundances challenges our understanding of chemical mixing processes. Such issues are clearly not confined to the Sun, with similar questions arising for many astrophysical bodies.

In situations where there is a clearly dominant mechanism (such as convection), theories of the transport (such as mixing length theory) have readily emerged. On the other hand, when extra mixing is required to explain observations in stellar radiative zones, where no dominant transport mechanism is apparent, a taxonomy of potential mixing processes has more gradually been unveiled. Perhaps the most notable recent advances concern processes introduced by rotational effects (rotational mixing), shear turbulence, double-diffusive convection, overshooting convection and gravity wave transport (see, e.g., Zahn 2008). The late Jean-Paul Zahn and collaborators published extensively on such work, and a perspective of the complexity of this taxonomy is afforded in Figure 1 of Mathis & Zahn (2005).

The role of the magnetic field in the dynamics of mixing can be two-fold. First, magnetic fields can potentially affect many of the proposed non-magnetic mixing processes. Magnetic fields often inhibit instabilities (see, e.g., Chandresekhar 1961) and also therefore their transport and mixing properties. The effect of magnetic fields is often therefore considered in this constraining context. Second, magnetic fields can be a source of in-

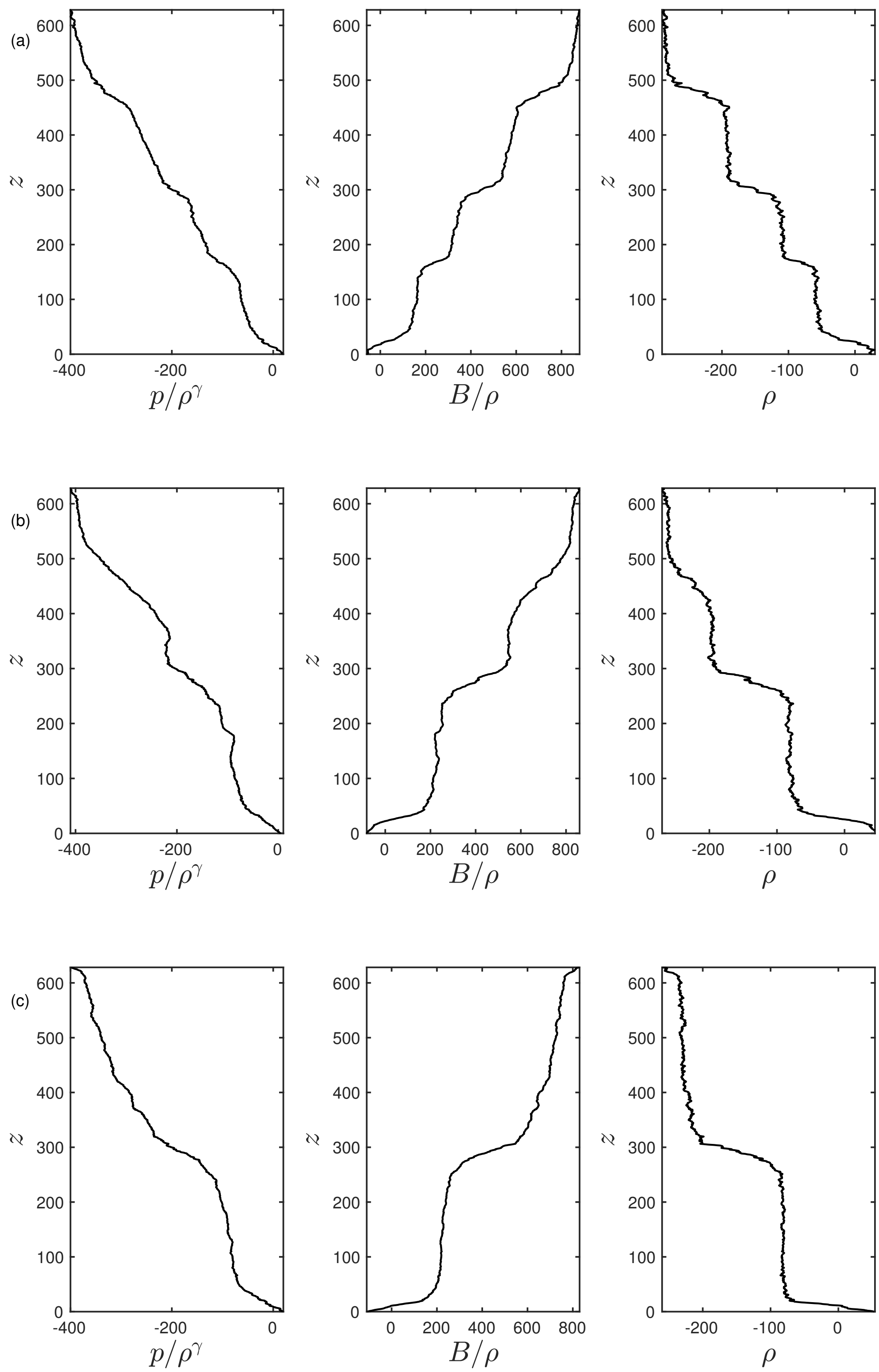

Figure 7. Horizontally averaged profiles of p/ρ^γ, B/ρ and ρ versus height at (a) $t = 3600$, (b) $t = 8050$, (c) $t = 11700$ (corresponding to the snapshots in Figures 3(c), 6a,b): $R_0^{-1} = 1.5$.

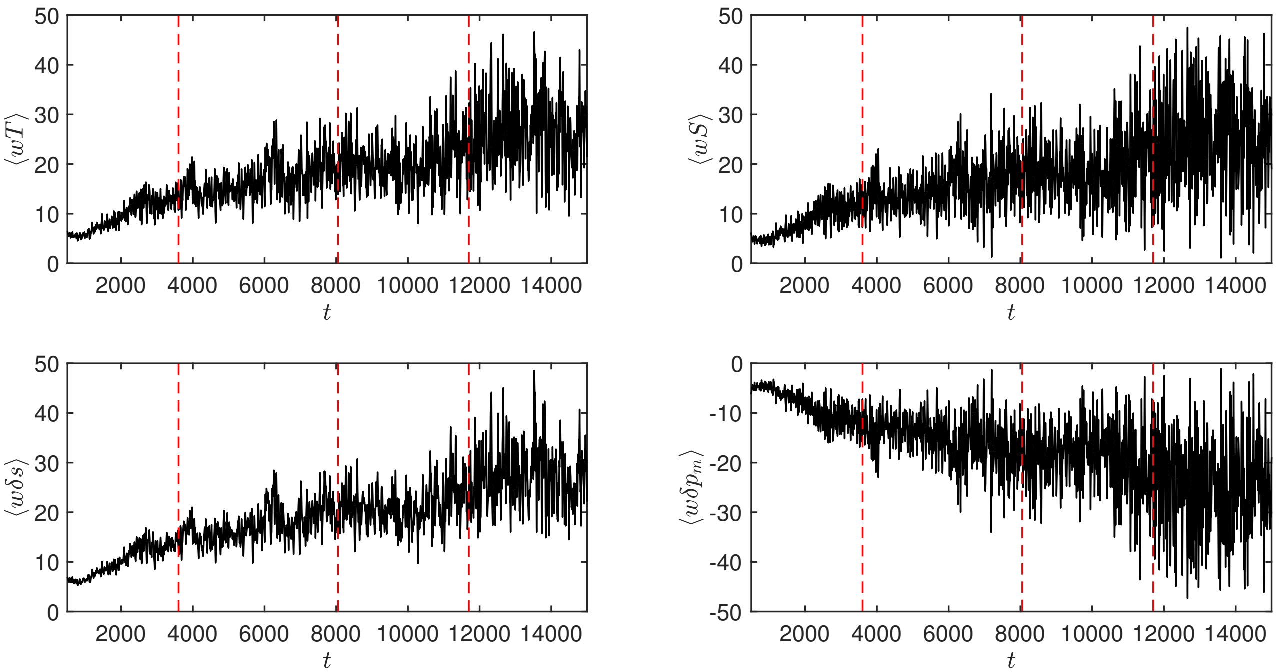

Figure 8. The top row shows the averaged vertical fluxes of T and S as a function of time, for all but the initial stages of the evolution, for the thermohaline problem with $R_0^{-1} = 1.5$. The bottom row shows the averaged vertical fluxes of δs and δp_m for the equivalent magnetic buoyancy problem. The dashed lines denote the times of the snapshots in Figures 3(c), 6(a,b).

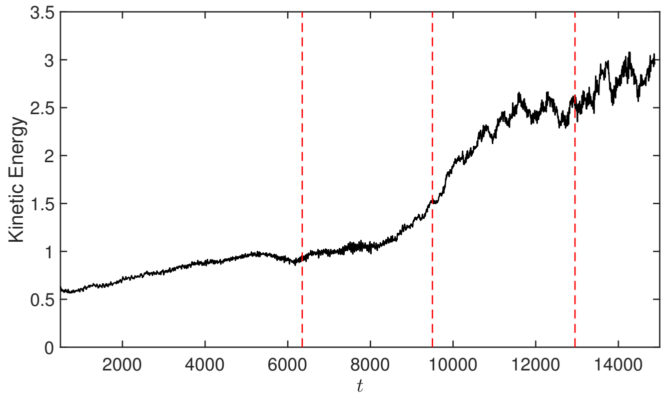

Figure 9. Kinetic energy as a function of time, for $t > 500$: $R_0^{-1} = 4$. The dashed lines denote the times of the snapshots in Figure 10.

stability themselves, thereby generating a further means of dynamical transport.

The latter context is the theme of this paper. Much of the research performed in this area has been directed at explaining the existence and geometry of observed magnetic fields. That is, the evolution and transport of the magnetic field itself has been the chief characteristic of interest, rather than any other induced mixing. For example, the stability and therefore the ultimate configuration of large-scale poloidal and toroidal fields in the deep interiors of stars has been investigated in a similar manner to the exploration of field configurations in plasma confinement devices (see, e.g., Markey & Tayler 1973; Pitts & Tayler 1985). Another substantial avenue of research has been devoted to dynamo instabilities (see, e.g., Moffatt & Dormy 2019). Generally driven by some combination of turbulence, rotation and shear, such instabilities can explain the initial generation of both small-scale and large-scale (mean) fields from weak seed fields, rather than the re-organization of large-scale fields as in Tayler instabilities. Magnetic buoyancy, the instability mechanism that is the subject of this paper, has been studied in the context of the creation and transport of compact magnetic flux structures from large-scale fields, in an effort to seek the origin of solar magnetic active regions and sunspots.

These examples all address the origin of certain magnetic field configurations rather than any induced transport of other ingredients, such as heat, angular momentum or chemical species. Perhaps the most well-known example in which magnetic field drives an instability that generates transport of another important quantity is the magneto-rotational instability (MRI), where the presence of a magnetic field instigates turbulence in an accretion disk, thereby allowing the turbulent transport of angular momentum and material (see, e.g., Balbus 2003). Another example that is more directly relevant to our study here is the work of Busso et al. (2007), which invokes magnetic buoyancy instabilities as a potential source of extra mixing (known in this context as 'cool bottom processing') to explain certain observed anomalies in low-mass red giant branch (RGB) and asymptotic giant branch (AGB) stars. Busso et al. (2007) ascribe the vertical transport required to explain the observations to the rise of thin buoyant flux tubes; they then infer the interior field strength necessary to produce these tubes at just the right rate to create the desired transport. Although only a phenomenological approach, this work ultimately imposes requirements on the interior fields that would lead to the necessary mixing. Our work is clearly directly relevant to this type of transport.

The overall aim of this paper has been to demonstrate that mixing induced by magnetic buoyancy instabilities could be a powerful and far more prevalent dynamical process than is currently widely recognized, and hence that it should be added to the overall catalogue of mixing processes. We have demonstrated that not only do magnetic buoyancy instabilities initiate extra mixing of magnetic and thermodynamic properties, but secondary instabilities to layered states can also significantly enhance that mixing. Furthermore, such mixing can be engendered under conditions that appear to be very stable in terms of the individual components.

In more detail, by exploiting the analogy derived by Spiegel & Weiss (1982), we have shown how the phenomenon of layering in thermosolutal convection implies the formation of layers in a system driven by magnetic buoyancy. In the astrophysically relevant regime in which the Prandtl number σ and diffusivity ratio τ are both small, the numerical evidence to date reveals that layering seems to occur more readily in the diffusive regime than in the fingering regime (Garaud 2018). In our translation of these results to the magnetic buoyancy case, we have thus concentrated on the diffusive regime. Although necessarily restricted to two-dimensional motions in pursuing the analogy, this has allowed us to conduct high resolution simulations in order to explore the regime of small σ and τ (though of course these are still much larger than the true astrophysical values). When both σ and τ are small, this leads to an enlarged region of instability (see expression (60)) and hence the potential for layering at higher values of R_0^{-1}.

In this paper, we have demonstrated, through numerical simulations, the formation of layers for $R_0^{-1} = 1.5$ and $R_0^{-1} = 4$ with $\sigma = \tau = 0.01$. From a thermohaline perspective, the two cases are very similar in many regards. However, when viewed from the magnetic perspective, the latter case is significant in that it falls in

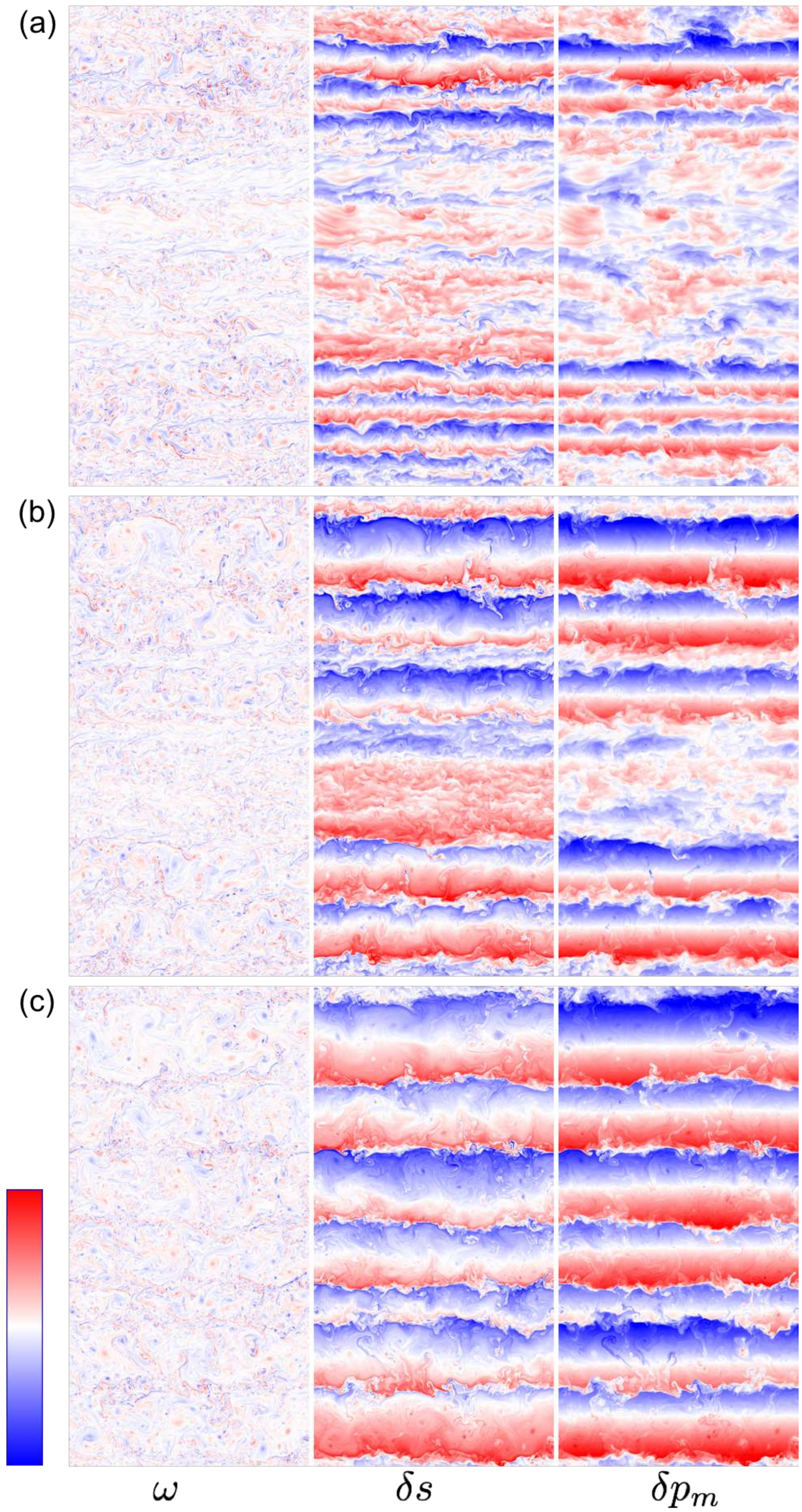

Figure 10. Snapshots at (a) $t = 6350$, (b) $t = 9500$ and (c) $t = 12950$ of ω, δs and δp_m (all scaled independently) for the case of $R_0^{-1} = 4$. The color table ranges from blue (largest negative value) to red (largest positive value), with white denoting the zero value.

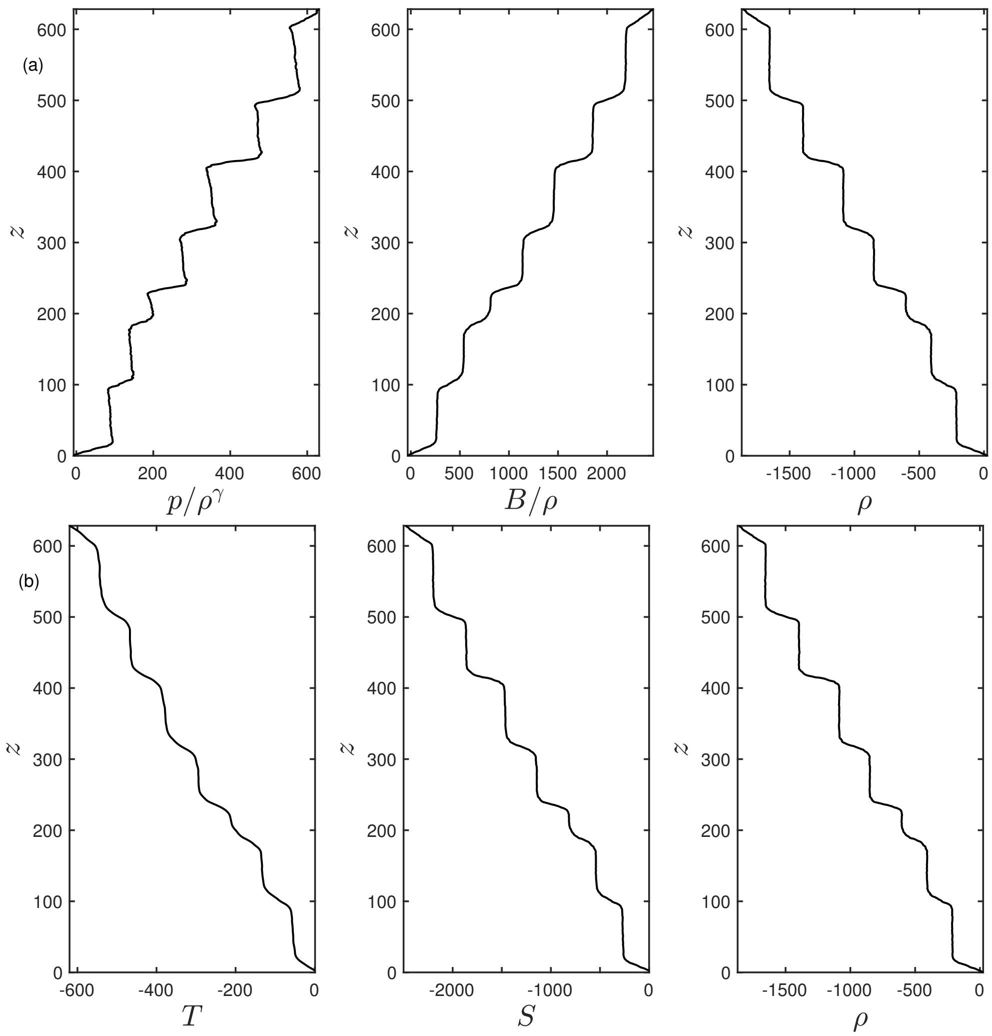

Figure 11. (a) Horizontally averaged profiles of p/ρ^γ, B/ρ and ρ versus height at $t = 12950$ (corresponding to the snapshots in Figure 10(c)): $R_0^{-1} = 4$. (b) The horizontally averaged profiles of T, S and ρ for the equivalent thermohaline problem.

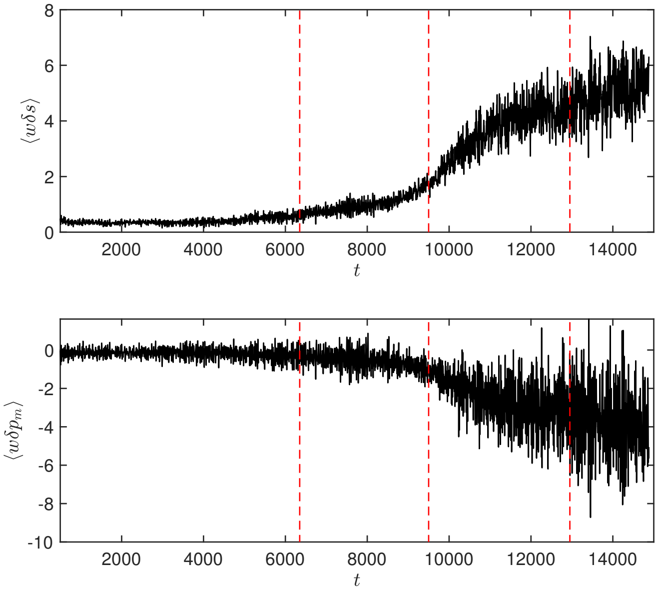

Figure 12. Averaged vertical fluxes of δs and δp_m as functions of time, for all but the initial stages of the evolution: $R_0^{-1} = 4$. The dashed lines denote the times of the snapshots in Figure 10.

what one might regard as the 'stable-stable' quadrant of magnetic buoyancy instabilities, where the system is described by a subadiabatic entropy gradient and by B/ρ decreasing with height (see Figure 1(b)). Thus, at first glance, one might not even expect instability in this regime, let alone layering. In each of these two cases, we have shown that the initial instability to simple vertical 'elevator' modes quickly gives way to turbulence, which subsequently evolves to layered states (see Figures 3, 6, 10). These then slowly merge to form wider and wider layers. As time progresses, each new scenario possesses stronger transport properties, with the layered states being significantly (5-6 times) more efficient than the more homogeneous state that emerges after the initial instability (see Figures 8, 12).

It is important to consider where magnetic layer formation and the associated enhanced transport may be of significance astrophysically. As shown in Figure 1, diffusive magnetic buoyancy instabilities are found in both the first and fourth quadrants in the (R_b, R_t) plane; furthermore, as we have demonstrated, the parameter regime of layer formation extends from close to the line of neutral stability in the first quadrant all the way into the fourth quadrant. In stellar convective zones, with strongly supercritical turbulent convection, magnetic buoyancy will presumably not be a major player. However, in radiative zones, where conditions are more quiescent and timescales much longer, there is the opportunity for magnetic buoyancy to act as the agent for layer formation. **For small values of σ and τ, and considering elevator modes, inequality (66) shows that with $\alpha > 0$ and $\beta > 0$, oscillatory convection occurs for**

$$R_2^{-1} \gtrsim \frac{\gamma}{(\gamma - 1)}, \tag{69}$$

or, in dimensional terms,

$$(\gamma - 1)\,\frac{ga^2}{c^2}\frac{\mathrm{d}}{\mathbf{d}z}\ln\left(\frac{B}{\rho}\right) > N^2 \tag{70}$$

(cf. inequality (8)). The magneto-Boussinesq approximation holds under the assumption that $a^2 \ll c^2$. Inequality (70) thus requires that for instability the subadiabatic gradient is smaller than the gradient of B/ρ. As explained by Corfield (1984) and Bowker et al. (2014), this condition is indeed necessary for asymptotic consistency of the magneto-Boussinesq approximation[2]. Application of inequality (70) to the Sun suggests that the most favorable conditions for oscillatory instability with $\alpha > 0$ and $\beta > 0$ will be towards the top of the radiative zone, where the subadiabatic gradient is indeed weak, and where the strong magnetic field in the overlying tachocline will inevitably lead, locally, to a magnetic field that increases with height. Although, it is hard to be definitive in asserting that layering will occur — owing to the impossibility of simulations in the astrophysical regime or the lack of a rigorous theory — we have shown unambiguously in § 4.2 that for small σ and τ (though not astrophysically small), pronounced layering does indeed occur with $\alpha > 0$ and $\beta > 0$ ($Rb > 0$, $Rt < 0$).

A non-solar application (but still drawing phenomenologically from our understanding of the solar radiative zone and tachocline dynamics) is provided by the study of Busso and collaborators (Busso et al. 2007), discussed above. Our work shows that the transport in a layered context is substantially greater than the simple advective transport associated with the small-scale magnetic structures that initially emerge, and hence may well be very different from that of highly conceptual flux tubes.

We conclude by considering future directions for the study of magnetic layering. Our approach in this study has been to exploit the analogy of Spiegel &

[2] To be precise, the magneto-Boussinesq approximation is based on an expansion in two small parameters: $\varepsilon_1 = d/H$ (H is scale height) and $\varepsilon_2 = \delta\rho/\rho_0$, with $\varepsilon_1 \gtrsim \varepsilon_2$. The ratio a^2/c^2 is $O(\varepsilon_2/\varepsilon_1)$ and the subadiabatic gradient is $O(\varepsilon_2)$, not $O(\varepsilon_1)$ as one might naively suppose.

Weiss (1982), thus allowing us to translate between two-dimensional thermohaline convection and interchange modes of magnetic buoyancy instability under the magneto-Boussinesq approximation. It is though important to look beyond the constraints imposed by the analogy. For thermohaline convection, the nature of two-dimensional versus three-dimensional simulations was investigated in some detail by Garaud & Brummell (2015). It was found that two-dimensional simulations of the diffusive case (as performed here) were reasonably representative of the full three-dimensional dynamics (although more care is definitely needed for the fingering case). More significantly, for the magnetic system in general, we expect similarities between the two- and three-dimensional evolutions since the basic state field imposes a preferred horizontal direction. The most readily excited linear mode of magnetic buoyancy instability, although three-dimensional, has a very long wavelength in the direction of the imposed field (see, e.g., Acheson 1979). Furthermore, the nonlinear evolution of three-dimensional magnetic buoyancy instabilities (Matthews et al 1995) has many features in common with that of two-dimensional (interchange) modes (Cattaneo & Hughes 1988). The most important consequence of relaxing the Boussinesq approximation (through considering either the anelastic approximation or the full compressible equations) is the introduction of a preferred lengthscale into the system, through, for example, the pressure scale height. It is clearly important to understand the influence of this scale on the layering and transport processes. **Also, in seeking more realism, it should be noted that, even in the extension to 3D, the current problem as set up only examines the instability of an initially unidirectional field, and more complex initial field geometries should be studied.**

Explaining the formation, maintenance and transport properties of layers is an area of intense current research, not just for double-diffusive systems, but in the contexts of forced stratified turbulence, of planetary jet formation (where the jets are manifestations of a potential vorticity staircase) and of the corrugated shear flow in fusion plasmas (the $\boldsymbol{E} \times \boldsymbol{B}$ staircase). There is still considerable debate over the underlying physical mechanisms and, indeed, whether there is a common thread between the different systems that exhibit layering. In terms of magnetic buoyancy layering, the important challenge ahead is to build upon the numerical simulations to devise a theoretical model valid in the regime $R_1^{-1} \gg 1, \sigma \ll 1, \tau \ll 1$ that can provide an estimate of where layering is to be expected and, in such cases, how the turbulent transport depends on the parameters of the problem.

We thank Pascale Garaud for many useful discussions. **We also thank the referee for a very insightful report, which helped improve the paper.** This research was supported by STFC grant ST/N000765/1, NSF AST grant 1908010 and NASA-NSF DRIVE Center Phase 1 grant 80NSSC20K0602 (subcontract to University of California, Santa Cruz). The computations were undertaken on the DiRAC@Durham facility managed by the Institute for Computational Cosmology on behalf of the STFC DiRAC HPC Facility (www.dirac.ac.uk), and also on the ARC High Performance Computing facilities at the University of Leeds. The DiRAC equipment was funded by BEIS capital funding via STFC capital grants ST/P002293/1, ST/R002371/1 and ST/S002502/1, Durham University and STFC operations grant ST/R000832/1. DiRAC is part of the National e-Infrastructure.

APPENDIX

A. DERIVATION OF EXPRESSIONS FOR p/ρ^γ, B/ρ AND $\hat{\rho}$

Here we provide the derivations of expressions (43), (44), (46) for p/ρ^γ, B/ρ and the density deviation $\hat{\rho}$. Under the Boussinesq approximation, in which scale heights of the basic state are large, we may approximate the basic state as being linear in z. Thus, to first order in small quantities, we may write, before any rescaling or non-dimensionalization,

$$\frac{p}{\rho^\gamma} = \frac{p_0}{\rho_0^\gamma} \left(1 + z \frac{\mathrm{d}}{\mathrm{d}z} \ln \left(\frac{p}{\rho^\gamma} \right) + \frac{\delta p}{p_0} - \gamma \frac{\delta \rho}{\rho_0} \right). \tag{A1}$$

Recall that, under the magneto-Boussinesq approximation, it is the variation in *total* pressure that is small, and, crucially, much smaller than the individual variations of the gas and magnetic pressures; i.e. $\delta p \approx -\delta p_m$. On using this result, together with the perfect gas law, expression (A1) can be written as

$$\frac{p}{\rho^\gamma} = \frac{p_0}{\rho_0^\gamma}\left(1 + z\frac{\mathrm{d}}{\mathrm{d}z}\ln\left(\frac{p}{\rho^\gamma}\right) + \gamma\frac{\delta T}{T_0} + (\gamma - 1)\frac{\delta p_m}{p_0}\right) \tag{A2}$$

$$= \frac{p_0}{\rho_0^\gamma}\left(1 + z\frac{\mathrm{d}}{\mathrm{d}z}\ln\left(\frac{p}{\rho^\gamma}\right) + \gamma\frac{\delta T^*}{T_0} + \frac{(\gamma - 1)}{(1-\tau)}\frac{\delta p_m}{p_0}\right), \tag{A3}$$

on using the definition for δT^*, given by (20).

The consistent scaling is to scale p/ρ^γ with $(p_0/\rho_0^\gamma)(d|\beta^*|/T_0)$, thus giving the dimensionless expression (43):

$$\frac{p}{\rho^\gamma} = \text{const.} + \left(\operatorname{sgn}(\beta^*)\gamma + \frac{\operatorname{sgn}(\alpha)}{R_1}\frac{(\gamma-1)}{(1-\tau)}\right)z + \gamma\frac{\delta T^*}{T_0} + \frac{(\gamma-1)}{(1-\tau)}\frac{\delta p_m}{p_0}. \tag{A4}$$

Thus for the *diffusive regime*, in which $\operatorname{sgn}(\alpha) = +1$ and $\operatorname{sgn}(\beta^*) = -1$, we obtain

$$\frac{p}{\rho^\gamma} = \text{const.} - \left(\gamma - \frac{1}{R_1}\frac{(\gamma-1)}{(1-\tau)}\right)z + \gamma\frac{\delta T^*}{T_0} + \frac{(\gamma-1)}{(1-\tau)}\frac{\delta p_m}{p_0}. \tag{A5}$$

Similarly, before any rescaling or non-dimensionalization, we can write,

$$\frac{B}{\rho} = \frac{B_0}{\rho_0}\left(1 + z\frac{\mathrm{d}}{\mathrm{d}z}\ln\left(\frac{B}{\rho}\right) + \frac{\delta p_m}{B_0^2/\mu_0}\right). \tag{A6}$$

Note that in the magneto-Boussinesq approximation, the term involving $\delta\rho$ is formally smaller (by a ratio of the square of the Alfvén speed to the square of the sound speed) and hence is neglected (see Hughes & Weiss 1995). Since we have chosen to scale δp_m with $|\beta^*|dp_0/T_0$, it is consistent to scale B/ρ with $|\beta^*|dp_0\mu_0/T_0B_0\rho_0$. This leads to the following expression for (dimensionless) B/ρ:

$$\frac{B}{\rho} = \text{const.} + \frac{\operatorname{sgn}(\alpha)}{R_1}z + \delta p_m. \tag{A7}$$

In the diffusive regime, this becomes

$$\frac{B}{\rho} = \text{const.} + \frac{1}{R_1}z + \delta p_m. \tag{A8}$$

In thermohaline convection, determining an expression for the overall density is straightforward. For magnetic buoyancy, it is a little more involved since the basic state density profile involves quantities that are not used in the scaling (unlike in thermohaline convection where the basic state density depends on the temperature and salinity profiles, which then go into R_0). To first order in small quantities, we may write

$$\rho = \rho_0\left(1 + z\frac{\mathrm{d}}{\mathrm{d}z}\ln\rho - \frac{\delta T}{T_0} - \frac{\delta p_m}{p_0}\right). \tag{A9}$$

We may express the equation for the magnetohydrostatic basic state,

$$\frac{\mathrm{d}}{\mathrm{d}z}\left(p + \frac{B^2}{2\mu_0}\right) = -\rho g, \tag{A10}$$

as

$$\left(\gamma + \frac{B^2}{2\mu_0 p}\right)\frac{\mathrm{d}\ln\rho}{\mathrm{d}z} = -\frac{\gamma\beta}{T_0} - \frac{\alpha}{p} - \frac{\rho g}{p}, \tag{A11}$$

where α and β are as defined in § 2.2. The second term in the bracket can be neglected (Alfvén speed $\ll$ sound speed). Thus expression (A9) becomes

$$\frac{\rho}{\rho_0} = 1 - \left(\frac{\beta}{T_0} + \frac{\alpha}{\gamma p} + \frac{\rho g}{\gamma p}\right)z - \frac{\delta T}{T_0} - \frac{\delta p_m}{p_0}. \tag{A12}$$

There is no straightforward way of dealing with the third term in the bracket, since it brings in quantities that are not used in the scalings of the variables. We therefore consider deviations away from the reference state defined by

$$\rho = \text{const.} - \frac{\rho_0^2 g}{\gamma p_0}z. \tag{A13}$$

If we denote the deviation from this state as $\hat{\rho}$ then

$$\frac{\hat{\rho}}{\rho_0} = -\left(\frac{\beta}{T_0} + \frac{\alpha}{\gamma p_0}\right) z - \frac{\delta T}{T_0} - \frac{\delta p_m}{p_0}. \tag{A14}$$

On substituting for β^* and δT^*, and scaling $\hat{\rho}$ with $d\rho_0|\beta^*|/T_0$, we obtain the following dimensionless expression for $\hat{\rho}$:

$$\hat{\rho} = -\left(\mathrm{sgn}(\beta^*) + \frac{(\gamma-\tau)}{\gamma(1-\tau)}\frac{\mathrm{sgn}(\alpha)}{R_1}\right) z - \delta T^* + \frac{(\gamma-\tau)}{\gamma(1-\tau)}\delta p_m. \tag{A15}$$

REFERENCES

Acheson, D. J. 1979, SoPh, 62, 23

Balbus, S. A. 2003, Ann. Rev. Astron. Astrophys., 41: 555597

Batiste, O., Knobloch, E., Alonso, A. & Mercader, I. 2006, JFM, 560, 149

Bowker, J.A., Hughes, D.W. & Kersalé, E. 2014, GApFD, 108, 553

Busso, M., Wasserburg, G.J., Noll, K.M & Calandra, A. 2007, ApJ, 671:802

Cattaneo, F. & Hughes, D. W. 1988, JFM, 196, 323

Chandrasekhar, S. 1961, Hydrodynamic and Hydromagnetic Stability (Oxford: Clarendon Press)

Corfield, C. N. 1984, GApFD, 29, 19

Garaud, P. 2018, Ann. Rev. Fluid Mech, 50, 275

Garaud, P. & Brummell, N.H. 2015, ApJ, 815, 42

Gilman, P. A. 1970, ApJ, 162, 1019

Gough, D. O. 2007, in The Solar Tachocline, ed. D. W. Hughes, R. Rosner, & N. O. Weiss (Cambridge: Cambridge Univ. Press), 3

Hughes, D.W. 1985, GApFD, 32, 273

Hughes, D. W. 2007, in The Solar Tachocline, ed. D. W. Hughes, R. Rosner, & N. O. Weiss (Cambridge: Cambridge Univ. Press), 275

Hughes, D. W., & Cattaneo, F. 1987, GApFD 39, 65

Hughes, D. W., & Proctor, M. R. E. 1988, AnRFM, 20, 187

Hughes, D. W., & Weiss, N. O. 1995, JFM, 301, 383

Langer, N. 1991, A&A, 252, 669

Markey, P. & Tayler, R.J. 1973, MNRAS, 173, 77

Mathis, S. & Zahn, J.-P. 2005, A&A, 440, 653

Matthews, P. C., Hughes, D. W., Proctor, M. R. E. 1995, ApJ, 448, 938

Merryfield, W. J. 2000, JPO, 30, 1046

Mirouh, G. M., Garaud, P., Stellmach, S., Traxler, A. L. Wood, T. S. 2012, ApJ, 750:61

Moffatt, H. K. & Dormy, E. 2019 Self-Exciting Fluid Dynamos (Cambridge: Cambridge University Press)

Newcomb, W. A. 1961, PhFl, 4, 391

Parker, E. N. 1966, ApJ, 145, 811

Phillips, O. M. 1972, DSR, 19, 79

Pitts, E. & Tayler, R.J. 1985, MNRAS, 216, 139

Posmentier, E. S. 1977, JPO, 7, 298

Radko, T. 2003, JFM, 497, 365

Radko, T. 2013, Double-Diffusive Convection (Cambridge: Cambridge University Press)

Rahmstorf, S. 2006, in Encyclopedia of Quaternary Sciences (ed. S. A. Elias) (Elsevier)

Rosenblum, E., Garaud, P., Traxler, A. & Stellmach, S. 2011, ApJ, 731:66

Schmitt, R. W. 1994, AnRFM, 26, 255

Schmitt, R. W., Ledwell, J.R., Montgomery, E.T., Polzin, K.L., Toole, J.M. 2005 Sci, 308, 685

Spiegel, E. A., & Veronis, G. 1960 ApJ, 131, 442

Spiegel, E. A., & Weiss, N. O. 1982, GApFD, 22, 219

Stellmach, S., Traxler, A., Garaud, P., Brummell, N. & Radko, T. 2011, JFM, 677, 554

Stern, M. E. 1969, JFM, 35, 209

Stern, M. E., & Radko, T. 1998, JMR, 56, 157

Thomas, J. H., & Nye, A. H. 1975, PhFl, 18, 490

Timmermans, M.-L., Toole, J., Proshutinsky, A., Krishfield, R. & Plueddemann, A. 2008, JPO, 38, 133

Turner, J. S. 1973, Buoyancy Effects in Fluids (Cambridge: Cambridge University Press)

Weiss, N. O. & Proctor, M. R. E. 2014, Magnetoconvection (Cambridge: Cambridge University Press)

Zahn, J.-P. 2008, in The Art of Modelling Stars in the 21st Century, Proc. IAU Symp. 252, ed. L. Deng & K.L. Chan

Zhurbas, V. M., & Ozmidov, R. V. 1983, IzAOP, 19, 977